



2005-07-08

Black Spaghetti: A Numerical Model of Gravitational Collapse in 4 + 1 Spacetime

Michael P. Christenson
Brigham Young University - Provo

Follow this and additional works at: <https://scholarsarchive.byu.edu/etd>

 Part of the [Astrophysics and Astronomy Commons](#), and the [Physics Commons](#)

BYU ScholarsArchive Citation

Christenson, Michael P., "Black Spaghetti: A Numerical Model of Gravitational Collapse in 4 + 1 Spacetime" (2005). *All Theses and Dissertations*. 537.

<https://scholarsarchive.byu.edu/etd/537>

This Thesis is brought to you for free and open access by BYU ScholarsArchive. It has been accepted for inclusion in All Theses and Dissertations by an authorized administrator of BYU ScholarsArchive. For more information, please contact scholarsarchive@byu.edu, ellen_amatangelo@byu.edu.

BLACK SPAGHETTI: A NUMERICAL MODEL OF
GRAVITATIONAL COLLAPSE IN
4 + 1 SPACETIME

by

Michael P. Christenson

A thesis submitted to the faculty of
Brigham Young University
in partial fulfillment of the requirements for the degree of
Master of Science

Department of Physics and Astronomy
Brigham Young University

August 2005

BRIGHAM YOUNG UNIVERSITY

GRADUATE COMMITTEE APPROVAL

of a thesis submitted by

Michael P. Christenson

This thesis has been read by each member of the following graduate committee and by majority vote has been found to be satisfactory.

Date

Eric W. Hirschmann, Chair

Date

Ross L. Spencer

Date

William E. Dibble

BRIGHAM YOUNG UNIVERSITY

As chair of the candidate's graduate committee, I have read the thesis of Michael P. Christenson in its final form and have found that (1) its format, citations, and bibliographical style are consistent and acceptable and fulfill university and department style requirements; (2) its illustrative materials including figures, tables, and charts are in place; and (3) the final manuscript is satisfactory to the graduate committee and is ready for submission to the university library.

Date

Eric W. Hirschmann
Chair, Graduate Committee

Accepted for the Department

Ross L. Spencer
Graduate Coordinator

Accepted for the College

G. Rex Bryce
Associate Dean
College of Physical and Mathematical Sciences

ABSTRACT

BLACK SPAGHETTI: A NUMERICAL MODEL OF GRAVITATIONAL COLLAPSE IN 4 + 1 SPACETIME

Michael P. Christenson

Department of Physics and Astronomy

Master of Science

We investigate spherically-symmetric gravitational collapse in the presence of a single “large” extra dimension through the use of analytical and numerical techniques.

This has bearing on higher-dimensional ideas concerning hypothetical objects called “black strings,” or black holes extending into an extra circular dimension, which dimension we herein label ζ . These putative objects were first seriously considered as elements of string theory but have relevance in simpler, higher-dimensional generalization of Einstein’s general relativity.

We assume a universe of topology $\mathcal{M}^2 \times \mathbf{S}^2 \times \mathbf{S}^1$ (where \mathcal{M}^2 is a two-dimensional Lorentzian manifold; \mathbf{S}^2 is the sphere; and \mathbf{S}^1 is the circle). We model the formation of a uniform black string via two modes—the collapse of a massless scalar field, and of pure gravitational waves consisting of (gaussian) distortions in the extra dimension.

We report on and discuss two aspects of the nonlinear dynamics, *viz.*, that in five dimensions larger-amplitude fields appear to collapse more slowly than their lower-amplitude cousins; and that ζ -wave collapse exhibits signs of self-similarity at the threshold between black string formation and dispersal of the collapsing fields.

ACKNOWLEDGEMENTS

A great big thanks to all who encouraged, pushed, and helped me to get this thing done, including but not limited to my parents, Peter and Karen Christenson; my sisters, brother, and sister-in-law; my advisor, Dr. Eric Hirschmann; our wonderful department secretary, Diann Sorenson; and Bishops LaMarr Nielsen and J. Lynn Jones of the BYU 210th ward, and Eugene W. Freedman of the BYU 38th ward.

Special kudos go to Mrs. Jane Caves for noticing mathematical talent where I saw none, to Mr. Herman Price for giving me my first glimpse into calculus, and to Mr. Kinsey Blomgren for making my first two physics classes so enjoyable, thereby confirming my desire to study same. I shudder to think of a “parallel universe” in which these souls did not affect me the way they did.

My future wife is she to whom this thesis is primarily dedicated. I did this for you, my love, whoever and wherever you are.

This thesis was originally typeset using $\text{T}_{\text{E}}\text{X}$; many thanks to L. Tychonievich and especially T. Nakata for their invaluable assistance in converting it to $\text{L}^{\text{A}}\text{T}_{\text{E}}\text{X}$.

Contents

List of Tables	x
List of Figures	xi
1 Preliminaries	1
1.1 Background and Introduction	1
1.1.1 Hyperdimensional Theories Through the Ages	1
1.1.2 Randall and Sundrum’s Braneworld Universe	3
1.1.3 Black Strings and Black Pearl Necklaces	6
1.1.4 Critical phenomena	8
1.1.5 The Work We Herein Present	10
1.2 Notes on Notation	11
2 Setting the Stage	13
2.1 A Review of Basic General Relativity	13
2.1.1 The Mathematics: Tensors and Coordinate Systems	13
2.1.2 The Physics: Matter Determines Geometry	16
2.2 Spherical and Other Symmetries	19
3 Plan of Attack	25
3.1 Roads Not Taken	25
3.1.1 Regularity Issues	28
3.2 Sliced Spacetime: The Best Thing Since Sliced Bread	32

3.2.1	The ADM Strategy	35
3.2.2	Isotropic Coordinates and a Conformal Slice	37
4	Molding the Equations Like Wet Clay	42
4.1	Non-zero Components of the Slice's Ricci Curvature	42
4.2	Constraints on α , \tilde{K}_ρ^ρ , and ψ	43
4.2.1	The Maximal Slicing Condition and a Constraint on α	43
4.2.2	Introducing Ω , and a Constraint on \tilde{K}_ρ^ρ	45
4.2.3	Introducing Π , and a Constraint on ψ	47
4.3	Evolution equations	49
4.3.1	Evolution of Metric Fields	49
4.3.2	Evolution of the matter fields	51
5	Supplementary Equations	53
5.1	Apparent Horizon	53
5.2	Black Hole Mass	57
6	The Main Equation Library	58
6.1	Evolution	58
6.2	Constraints	59
6.3	Supplementary	59
7	Numerical Approach	60
7.1	Discretizing Derivatives Into Differences	60
7.1.1	Evolution	60
7.1.2	Constraints	62
7.2	Boundary Conditions	64
7.3	Convergence Testing	70

8	Results and Interpretations	73
8.1	Scalar Field Collapse	74
8.2	Gravitational Field Collapse	75
9	Some Final Words	85
9.1	Cosmological Considerations	85
9.2	Future Work	85
9.3	Summary and Conclusion	87
A	Fun with conformal metrics	90
	Bibliography	93

List of Tables

Table 1	
Notation rules	11
Table 2	
Criticality window for ϕ_0 at different resolutions	74
Table 3	
Criticality window for σ_0 at different resolutions	75

List of Figures

1.1	The braneworld scenario	4
2.1	Illustration of contravariant components in oblique axes	14
2.2	Illustration of covariant components in oblique axes	15
7.1	The convergence test result for σ at id3, id4, and id5	72
8.1	Semilog plot of $\sigma(t, \rho)$ for three initial amplitudes	78
8.2	Semilog plot of $\alpha(t, \rho)$ for three initial amplitudes	79
8.3	Time plot of $\sigma _{\rho=0}$ for three initial amplitudes	80
8.4	Time plot of $\alpha _{\rho=0}$ for three initial amplitudes	81
8.5	The supercritical and subcritical evolutions of σ	82
8.6	The supercritical and subcritical evolutions of α	83
8.7	Time plot of $\alpha _{\rho=0}$ for supercritical and subcritical evolutions	84

Chapter 1

Preliminaries

1.1 Background and Introduction

The possibility of higher-dimensional spacetimes becomes an interesting idea from the moment one first learns, from special relativity, that time is a “fourth dimension.” Questions such as “What would a higher-dimensional universe look like? Would gravity behave differently there?” and “Can we tell if there are more dimensions? If so, how?” rise unbidden from these naïve ponderances.

It turns out that in this case childlike naiveté might just be intuition in disguise. For, from Kaluza and Klein’s five-dimensional attempt at unifying electrodynamics with the spacetime metric [1] to string theorists’ ten-fold universe, to recent sensitive experiments in search of deviations from Newton’s inverse-square law [2,3], physicists have not shied away from entertaining hyperdimensional theories in their quest for a comprehensive understanding of fundamental forces.

1.1.1 Hyperdimensional Theories Through the Ages

The present era’s study of spacetimes with more dimensions than the 3+1 universe of “normal” general relativity formally began in the 1920’s—not too long after GR’s original publication by Einstein, and its stunning confirmation in the solar eclipse of 1919—when Kaluza and Klein (KK) proposed a five-dimensional model to unify gravity and electrodynamics [1]. Their idea, tempting in its simplicity but disappointing

in its reality, was to expand the 4-dimensional metric of gravity to a 5-dimensional metric that included the usual four-dimensional metric as a sub-matrix. In addition, one could interpret the larger manifold as including the four-vector potential $A^\mu = (V/c; \vec{A})$ which describes electromagnetism, and an additional scalar field, χ . Schematically it would take the form:

$$M_{ab} = \begin{pmatrix} g_{\mu\nu} \delta_{ab}^{\mu\nu} & A_\mu \delta_a^\mu \\ A_\nu \delta_b^\nu & \chi \end{pmatrix} \quad (1.1)$$

The beauty of this approach is that it describes both gravity and one of the other fundamental forces as purely geometrical effects; for, if M_{ab} is used as the metric in making the corresponding five-dimensional Ricci tensor, one miraculously produces the Einstein equations with the correct electromagnetic stress tensor, as well as the Maxwell equations. Such beauty is hard to dismiss as mere coincidence.

The great question that emerges from this consideration is, What *is* this extra or fifth dimension above and beyond the 3 + 1 to which we are accustomed, whose geometrical distortion is responsible for electrodynamics? In the original KK idea, this extra dimension was—somewhat arbitrarily—chosen to have the topology of a circle, *i.e.*, to be a compact dimension. There is, however, no apparent physical basis for making this choice.

Unfortunately, this combination of the spacetime metric with the electromagnetic four-potential, as well as other generalizations of the KK idea, have at least one significant failure in that they introduce complications and scalar fields that have not been observed experimentally. This is manifest in (1.1) with the introduction of the mysterious field, $M_{55} = \chi$, a massless scalar field, often called the dilaton. In the full KK equations, χ appears alongside the gravitational and electromagnetic fields and is

nontrivially coupled with them. Thus, notwithstanding the allure of the Kaluza-Klein hypothesis, it does not satisfy Einstein’s hope for a grand unification as neatly as one might hope.

Since the original innovation of KK, there have been various attempts to incorporate or resurrect their idea of geometrizing fundamental interactions in Einstein’s as-yet ill-fated quest. This is particularly true in recent years with the rise and various resurgences of string theory. Some of these models allow for higher-dimensional spacetimes with many more dimensions than the four that we perceive. For example, some models require as many as 10 or 11 dimensions. An unresolved issue in string theory is why we cannot sense any dimensions beyond the four with which we are familiar. One idea to account for our inability to measure them is that, as in the KK idea, those dimensions are “compactified” to some very small scale, perhaps on the order of the Planck length ($L_P \equiv \sqrt{G\hbar/c^3} \sim 10^{-35}$ m). The energies required to probe such tiny spaces stretch far beyond our current technological capacity and taxpayer patience.

1.1.2 Randall and Sundrum’s Braneworld Universe

In 1999, Randall and Sundrum (RS) imported aspects of string theory into the cosmological arena [4,5]. They proposed that theories with extra dimensions were not *restricted* to being compactified (as by then had become the common assumption) and so could, in principle, feature dimensions of macroscopic size. Although the hypothesis that higher-dimensional theories could have *non*-compactified extra dimensions had been toyed with before [*e.g.* 6,7], RS proposed the first apparently internally self-consistent model. Most intriguingly, their proposal posited the idea that our visible universe was confined to a “brane,” or a codimension-one submanifold, within a larger manifold which has since come to be known as the “bulk.”

One may visualize such a universe as a piece of tissue paper (representing the brane) embedded in a vat of gelatin (bulk), as shown in Figure 1.1.

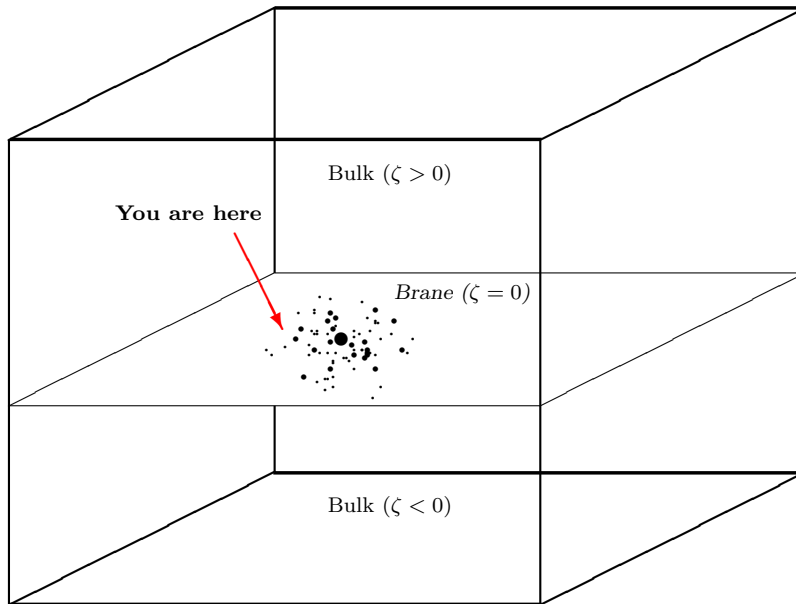


Figure 1.1 — The braneworld scenario: all matter and nongravitational bosons live at $\zeta = 0$, *i.e.*, on the brane. Gravity, being geometrical in nature, affects the bulk—which then produces nontraditional effects on the brane.

In the brane-universe the three interactions of the standard model are supposed to take place on the brane (corresponding to the tissue in our metaphor); whereas gravity, still considered as the effect of a warped spacetime, is under no such restriction and therefore acts in the full bulk (gelatin) or larger spacetime manifold—with interesting nontraditional effects on the brane.

Mathematically speaking, one assumes that the Einstein equations hold just as well in five dimensions as they do in four—indeed, that it is from the vantage-point of the five-dimensional observer that the pure “curvature equals stuff” theory holds true, whereas from the perspective of the lower dimensions (the braneworld) there are extra terms that enter the equations. For brane theory the relevant equations were obtained by Shiromizu, et al., [8]. These equations include two “exotic” extra pieces: a term quadratic in the four-dimensional stress tensor, and a tensor that represents

the back-reaction of gravitational action in the bulk onto the brane.

The physical interpretation of the Shiromizu-Einstein equations is as follows. Gravity on the brane would depend upon the matter and energy on the brane itself in the usual way at low-energy states. In addition, gravity would be especially sensitive to extreme conditions, such as a black hole, which the quadratic term would emphasize. Furthermore, it would be modified by distortions in the bulk. The latter point is especially well-illustrated in our mental image of tissue paper in gelatin.

In the flurry of research following this bold proposal, the majority of the work done has been to obtain *static* or *cosmological* solutions to the Shiromizu-Einstein equations or variations thereof, and investigations of linear perturbations of known 4-D metrics in the presence of the bulk [*e.g.* 9,10].

Some important questions with regard to these “braneworld” models touch on their time-dependent, evolutionary properties. For example, are the known static brane-solutions stable? Do cosmological perturbations remain small? What does gravitational collapse in braneworlds look like, and how is it influenced by the bulk? Can stable objects, *i.e.* stars and black holes, be formed on the brane? How far to black holes and other gravitating object extend into the bulk? Our original intent had been to address questions such as these.

Since the analytical aspects of the problem would involve solving a complicated set of second-order nonlinear coupled PDEs in three dimensions, we thought to apply numerical techniques to evolve the *dynamics* of *local* black hole formation on the brane. However, as we pondered how to coax brane-friendly boundary conditions from W. Israel’s treatment of dust shells [11], Hirschmann and Wang [12] showed that there existed a strong possibility that braneworlds must be either static or spatially uniform—respectively dooming the dynamic creation or the existence of black holes, as well as all other spatially or temporally local variations in the universe (*e.g.*,

galaxies, stars, planets, us).

1.1.3 Black Strings and Black Pearl Necklaces

This negative result made it difficult to proceed with any confidence of finding a viable solution to the question of braneworld black hole dynamics. An alternative (which we had previously considered) was to abandon the brane and consider the dynamics of a generic five-dimensional gravitational theory. While no longer an outgrowth of the RS model, this still considers ideas coming from KK or string-like theories.

One variant on these latter theories is the existence of higher-dimensional “black objects.” The simplest specimen is the four-dimensional Schwarzschild black hole topologically crossed with \mathbf{S}^1 (the circle). The object thus formed could therefore be described as a “black string,” which shall henceforth be our terminology. This geometry, which possesses a regular event horizon, satisfies the five-dimensional vacuum Einstein equations. This simple solution has generalizations in various string theories; understanding its dynamics might help in understanding various aspects of string theory. Likewise, although this solution is not specifically a braneworld solution, one might imagine (despite the above negative result) that in more complicated braneworld scenarios one might also find analogous extended black objects. Therefore much of what has been done in RS brane theory could have¹ carried over into black strings, since the brane was to assert itself mainly in the imposition of boundary conditions.

With this motivation, coming from both string theory and braneworlds, it is worthwhile trying to gain a more complete understanding of black strings. For instance, one question that persists from brane-land concerns stability properties. In the 1960’s and

¹ I say “could have” because using the braneworld equations was not the approach we ultimately took.

70’s considerable work was done to prove that the classical $3 + 1$ Schwarzschild and Kerr solutions in four-dimensional general relativity were in fact stable with respect to small perturbations. This meant that such objects—which at the time did not enjoy the widespread acceptance in the physics community we now take for granted—could in fact be the end-state of gravitational collapse. It is natural, therefore, to apply a similar analysis to the question of black string stability. This question was first addressed perturbatively by Gregory and Laflamme [13,14].

They showed that for a simple black string (which is, by reminder, just the Schwarzschild black hole $\times \mathbf{S}^1$ in five dimensions) with a length in the extra (ζ) direction larger than the black hole’s spherical radius, one could expect the black string (which they more deliciously referred to as a “black doughnut”) to be unstable: their calculation revealed an exponentially growing mode that would render the static, translationally (in ζ) invariant solution unstable.

Although this was a perturbative calculation, and therefore unable to say exactly what the end-state of this instability would be, the authors conjectured in [13] that the initially smooth black string would “bead up” into what we’d call a “black pearl necklace”—that the horizon, which initially possesses translational invariance, would in fact pinch off in regular intervals, and one would be left with a series of 5-D black holes in the ζ direction. Some results in string theory actually depend upon this conjectured dynamical instability [15-18], and so there is some importance to establishing it definitively.

Adding to the consternation, however, Horowitz and Maeda in [19] present an argument that, while the instability drives the initially smooth black string away from a translationally-invariant (in ζ) state, the pinch-off never actually occurs. Using global techniques and the Raychaudhuri equation (adapted to five dimensions) they were able to show that the horizon cannot bifurcate in finite affine parameter (or

“time”). This is a provocative result, given the earlier conjecture and the various results that seem to depend upon the occurrence of pinch-offs.

Then again, as recently as this past April (2005), Marolf [20] suggested that Horowitz and Maeda [19] were mistaken; that indeed “pinch-off at a finite advanced time is in fact a *natural* expectation of the bounds derived by Horowitz and Maeda.”

Nor has this investigation been the sole province of analytical theorists. As had been suggested early on by Horowitz [21], the general nonlinear evolution of the black string should be as amenable to numerical techniques as are the linear perturbative calculations. Indeed, if one considers possible spatial dependence in the radial and ζ -directions only, the problem amounts to writing a 2 + 1 evolution code that solves Einstein’s equations in cylindrical-like coordinates.

This was done with partial success by Choptuik, et al. [22], who wrote an evolution code using a simple black string as its initial data. Calculating geometric quantities such as the ratios of large and small circumferences, they were able to confirm the instability’s existence and in fact measure its rate of growth. However, their code was not sufficiently robust to determine the final end-state of the black string. While they saw indications of continued growth in the ratio of the largest to the smallest circumferences around the black string, they were unable to determine definitively whether that growth lead to the pinch-off of the horizon. Thus the larger question, pertaining to the end-state of a black string, remains unanswered. (As a result, both sides claim vindication of their ideas.)

1.1.4 Critical phenomena

As computational relativity came into its own it was found [23], and replicated many times over in every conceivable construct [24], that black hole formation follows a rule that is at once intuitive and completely unexpected. Intuitively, if one has a lot

of “stuff” (typically a scalar field)—meaning, if any one of the scalar field amplitude ϕ_0 , the width δ_ϕ , or the mean radius ρ_0 in an initial gaussian scalar-field profile $\phi = \phi_0 \exp [-(\rho - \rho_0)^2/\delta_\phi^2]$ is sufficiently large—a black hole of a certain mass is the end result. The greater the initial parameter in question (which is commonly given the generic label p), the greater the mass of the resulting black hole. It is likewise intuitive that if these quantities are sufficiently small, no black hole is formed.

Naturally one begins to wonder where in initial-field-phase-space the black-hole-ness “turns on,” and whether the mass-dependence of the black hole continues all the way down to zero. The answer, which by now has attained almost to the stature of common knowledge (at least, within the numerical relativity community), is something that seems to defy intuition: black hole mass scales according to the rule

$$m_{\text{BH}} \propto (p - p^*)^\gamma \tag{1.2}$$

where $\gamma \approx 0.374$ is an apparently universal constant, as it is the same for any one-parameter family of scalar field, and does not depend on which parameter ($\phi_0, \delta_\phi, \rho_0$) is used; $p^* > 0$ is the critical value of the initial parameter. This means that the mass of the resulting black hole (a) does not increase linearly with p but *is* asymptotically unbounded; and (b) is continuous with the no-black-hole state at $p = p^*, m_{\text{BH}} = 0$, although it comes in at infinite slope (which implies that the formation of a black hole will be extremely sensitive to small variations in p near p^*). At criticality, therefore, massless black holes become a possibility.

Even more remarkably, for p very close to the critical point, $p = (1 \pm \varepsilon)p^*$, the fields exhibit self-similarity. Further work [24] shows that this self-echoing structure can be either continuous or discrete, and that it is no numerical mirage, but can be obtained analytically with prudent coordinate choices.

1.1.5 The Work We Herein Present

The work that will be discussed herein is in some sense a reconsideration and simplification of the black-string end-state problem. While solving the full problem is compelling, and something which we'd like to eventually do, we here limit our discussion to an attempt to solve a simpler $1 + 1$ dimensional black string evolution problem.

While disappointing from the perspective of looking for the final state of the instability, our motivation is to learn something about five-dimensional gravity on a fundamental level: the effect that the mere existence of an extra spatial dimension might have upon the evolution and final product of gravitational collapse. The problem remains dynamic, albeit not in the ζ direction; in fact, the extra dimension allows for not only scalar field collapse, but also the collapse of pure gravitational waves which replicate, in five dimensions, the fascinating “critical phenomena” found in $3 + 1$ spacetime gravitational collapse.

Our hope, then, would be that once we have a better understanding of the dynamics in this simplified model problem, we might be able to extend our approach to the more involved $2 + 1$ case. Along these lines, it is interesting to note [25] that the Choquet group was unable to successfully model gravitational collapse of a scalar field to a black string.

Solving Einstein's second order coupled nonlinear partial differential equations is never a walk in the park, even under the best of circumstances. General, exact, closed-form solutions have eluded physicists since the equations were first published in 1915. Our approach, then, will be as follows. We will assume spherical and ζ -translation symmetry, and our only coordinate dependence will be on a conformally defined radial coordinate and a time coordinate. We will of course need the equations of motion for the matter, in addition to the Einstein equations. To perform a

time evolution we will make the standard splitting of space and time of Arnowitt, Deser, and Misner (ADM) [26]. One route to this separation includes dividing out the spherical symmetry already present and viewing the system as KK-like reduced fields on some submanifold of the full spacetime. While attractive conceptually (and still useful in some ways), we discovered that there are implementation issues on the numerical side. The ADM method, then, will be augmented by a careful study of regularity conditions. We believe that careful treatment of, for example, the symmetry axis, permits us to build a stable evolution—a crucial requirement of any numerical code. Indeed, we feel we have an important technical result regarding regularity and coordinate conditions which should play a role in the more general $2 + 1$ case as well.

In subsequent sections of this thesis we will discuss in detail the meaning of our assumed symmetries, the equations that we solve, regularity conditions, and the results of our simulations.

1.2 Notes on Notation

In dealing with equations pertaining to manifolds of diverse dimensionality, it becomes most helpful to assign specific meaning to the letters to be used as tensor component indices and to use different symbols for the various metrics and their corresponding covariant differential operators. Therefore, in what follows we will rigorously enforce the rules summarized in Table 1.

Manifold	Coordinates	Metric	Indices	Operator
Universe	$(t, \rho, \zeta, \theta, \varphi)$	$g_{\mu\nu}$	$\alpha, \beta, \gamma, \dots$	∇_{μ}
$2 + 1$ spacetime	(t, ρ, ζ)	\tilde{g}_{ab}	a, b, c, \dots	D_a
Unit sphere	(θ, φ)	σ_{mn}	l, m, n, \dots	—
$4 + 0$ spatial slice	$(\rho, \zeta, \theta, \varphi)$	γ_{AB}	A, B, C, \dots	Δ_A
Trapped surface	(ζ, θ, φ)	\hat{g}_{AB}	$\mathcal{A}, \mathcal{B}, \mathcal{C}, \dots$	—

Table 1

Other notations may be introduced as needed. As per established customs, commas denote partial differentiation ($f_{,\mu} = \partial_\mu f = \frac{\partial f}{\partial x^\mu}$), the determinant of a metric is denoted by its alphabetic name without any indices ($g = \det[g_{\mu\nu}]$), and the summation convention is in force throughout (all pairwise repeated indices are summed: $a^\mu b_\mu = \sum_\mu a^\mu b_\mu$). Also, at a later point we will find it convenient to use primes and overdots to denote derivatives with respect to ρ and t , respectively.

Chapter 2

Setting the Stage

2.1 A Review of Basic General Relativity

2.1.1 The Mathematics: Tensors and Coordinate Systems

General relativity is, as the name suggests, a generalization of the special relativity introduced by Einstein in 1905. In mathematical parlance this requires that the theory be “generally covariant,” or in other words, that it be formulated in terms of tensors. A tensor is an organized collection of quantities (if they are functions, the object is said to be a tensor *field*) whose components obey a particularly simple transformation law between coordinate systems:

$$\bar{T}_{\mu\nu\dots}^{\alpha\beta\dots} = \frac{\partial x^\xi}{\partial \bar{x}^\mu} \frac{\partial x^\eta}{\partial \bar{x}^\nu} \dots \frac{\partial \bar{x}^\alpha}{\partial x^\gamma} \frac{\partial \bar{x}^\beta}{\partial x^\delta} \dots T_{\xi\eta\dots}^{\gamma\delta\dots} \quad (2.1)$$

This may look complicated, and hardly a way to “define” something as exotic as a tensor. Put simply, though, this definition simply tells us that *a tensor is a sum of tensors* in much the same way that “a vector is a sum of vectors” ($\mathbf{v} = v_k \vec{e}^k$) [27]. The number of indices, or the number of matrices required for a coordinate transformation, is called the tensor’s rank. A vector is also a tensor, of rank unity; scalars are rank-0 tensors (also called “invariants” because, aside from having to express their functional dependence in terms of the new coordinates, they remain unchanged under coordinate transformations). Most of general relativity concerns itself with rank-two tensors.

The components of a tensor are indexed according to their corresponding coordinates, and according to the type of basis used to build the coordinate system in which they are expressed. A component is said to be “contravariant” if the basis is defined as the direction of increasing x^μ , $\vec{e}_\mu \sim \partial_\mu$ (Fig. 2.1a). On the other hand, a component is called “covariant” if the basis used is tangential to the coordinate axis, $\vec{e}^\nu \sim dx^\nu$ (Fig. 2.2a). Contra- and covariant components are denoted by super- and subscripted indices, respectively, to wit: $\mathbf{T} = \vec{e}^\nu \cdots \vec{e}_\mu \cdots T_{\nu \dots}^{\mu \dots}$.

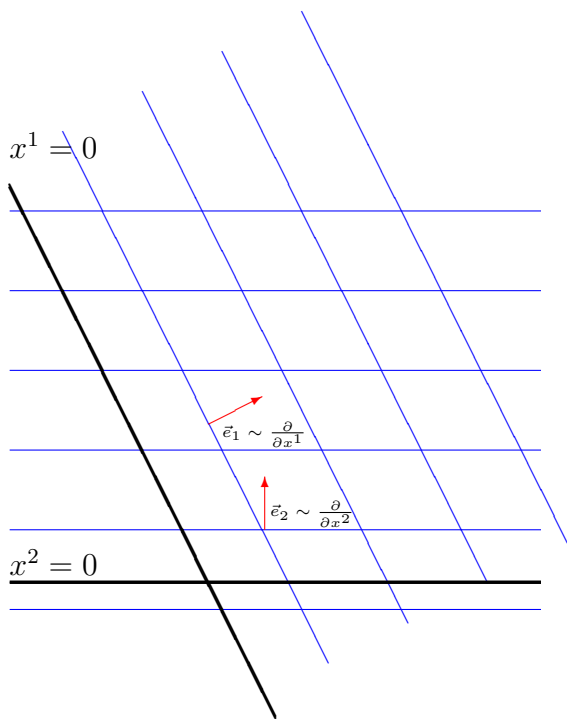


Figure 2.1a

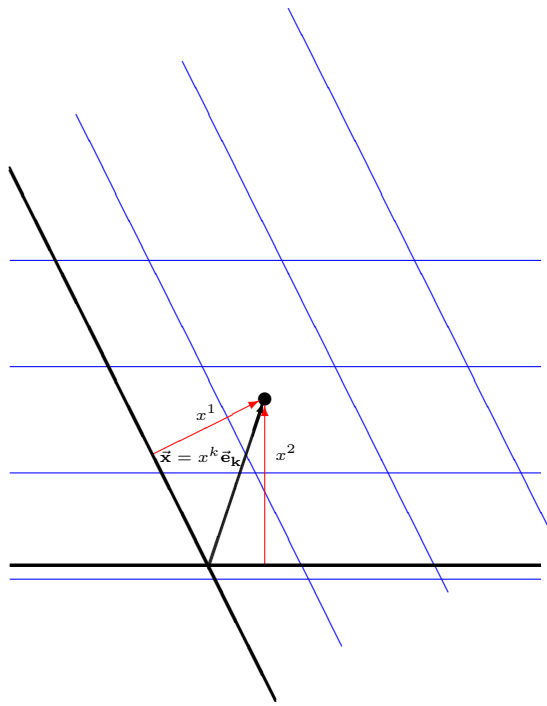


Figure 2.1b

Figure 2.1 — Illustration showing the contravariant basis vectors and components of a displacement vector in oblique axes. Figure 2.1a shows lines of constant x^k to which the respective contravariant basis vectors \vec{e}_k are perpendicular. Figure 2.1b illustrates that contravariant components of the vector \mathbf{x} are the coefficients in that linear combination $x^k \vec{e}_k$ which reproduces the vector itself.

The distinction between covariant and contravariant components is clearly unimportant in rectilinear coordinate systems (wherein $\vec{e}_\mu = \vec{e}^\mu = \{\hat{\mathbf{i}}, \hat{\mathbf{j}}, \hat{\mathbf{k}}\}$), which is why

its discussion is usually limited to a non-Euclidean context—although it could be an important consideration when a problem lends itself to oblique axes, as illustrated in Figures 2.1 and 2.2. Position, for instance, in a such a coordinate system could be measured with equal validity parallel to the axes (dx^μ), or perpendicular (∂_μ).

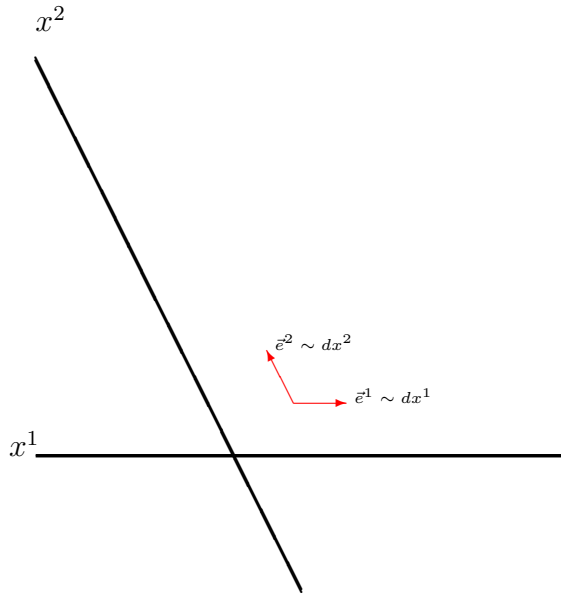


Figure 2.2a

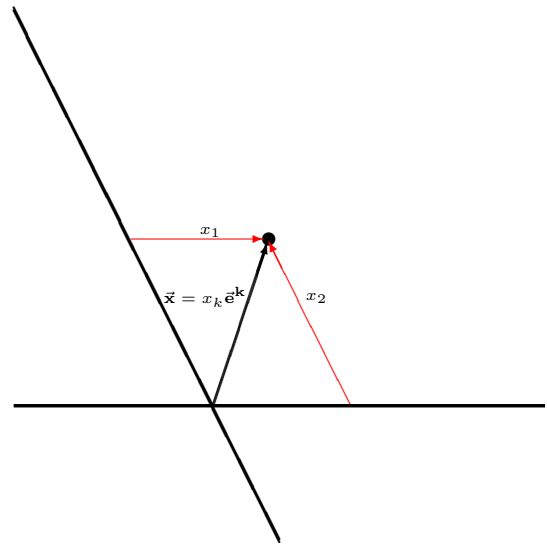


Figure 2.2b

Figure 2.2 — Illustration showing the covariant basis vectors and components of a displacement vector in oblique axes. Figure 2.2a shows how the covariant basis vectors \vec{e}^k are parallel to the coordinate axes. Figure 2.2b illustrates that covariant components of the vector \mathbf{x} are the coefficients in that linear combination $x_k \vec{e}^k$ which reproduces the vector itself.

2.1.2 The Physics: Matter Determines Geometry

Most of the tensors that play important roles in general relativity are of second rank. For example, the invariant interval between two infinitesimally separated point-events is given by

$$ds^2 = g_{\mu\nu} dx^\mu dx^\nu, \quad (2.2)$$

in which the rank-two tensor $g_{\mu\nu}$ is called the metric. The goal in general relativity is to use the Einstein equations to discover the functional form of the metric, given a certain mass-energy distribution.¹ It is akin to solving the Poisson equation, $\nabla^2\phi = 4\pi\rho$, for the gravitational potential ϕ , given a mass distribution ρ . In that sense, the erst-while purely geometrical components of $g_{\mu\nu}$ are endowed with a physical meaning as a set of gravitational potentials.

The metric tells us important things about the structure of spacetime, from the presence of singularities and event horizons in extreme (black hole) situations, to the more pedestrian gravitational “force” exhibited in the geodesic or covariant free-fall equation,

$$u^\nu \nabla_\nu u^\mu = \frac{d^2 x^\mu}{ds^2} + \Gamma_{\nu\lambda}^\mu \frac{dx^\nu}{ds} \frac{dx^\lambda}{ds} = 0, \quad (2.3)$$

where $u^\mu = \frac{dx^\mu}{ds}$ is the proper four-velocity. Here we have rather glibly made use of covariant differentiation,

$$\nabla_\alpha T_{\nu\dots}^{\mu\dots} \equiv \partial_\alpha T_{\nu\dots}^{\mu\dots} + \Gamma_{\alpha\beta}^\mu T_{\nu\dots}^{\beta\dots} \dots - \Gamma_{\alpha\nu}^\beta T_{\beta\dots}^{\mu\dots} \dots \dots \quad (2.4)$$

The $\Gamma_{\nu\lambda}^\mu$ are the metric connections or Christoffel symbols of the second kind, and are defined as a particular combination of partial derivatives of the metric:

$$\Gamma_{\mu\nu}^\sigma = \frac{1}{2} g^{\sigma\lambda} (g_{\mu\lambda,\nu} + g_{\lambda\nu,\mu} - g_{\mu\nu,\lambda}).$$

¹ Interestingly, originally it was thought better to use Einstein’s field equations in reverse, that is, to propose a metric, and find the matter field that would give such a spacetime—which may be why it fell to a young Karl Schwarzschild to find the first nontrivial solution. See [28].

The Christoffel symbols are an example of an indexed quantity that is not a tensor; $\Gamma_{\nu\lambda}^{\mu}$ does not follow the transformation law (2.1).

The Einstein equations themselves may be obtained by making a careful translation of Newtonian tidal effects into covariant language, but it is more straightforward to apply an action principle and a tensorial version of the calculus of variations. The action we will thus consider consists of a (5-D) gravitational piece and a piece representing the matter. In the case of a massless scalar field ϕ , the action will be:

$$\begin{aligned} S &= \int (\mathcal{L}_G + \kappa \mathcal{L}_M) d^5x \\ &= \int \left({}^{(5)}R - \kappa \partial_{\mu}\phi \partial^{\mu}\phi \right) \sqrt{-g} d^5x. \end{aligned} \quad (2.5)$$

(We could have included a cosmological term, but despite what cosmologists now tell us [29], the cosmological constant will remain equal to zero for the duration of our investigation.)

When varied with respect to the metric, the action S yields the famous Einstein equations:

$$G_{\mu\nu} = \kappa T_{\mu\nu} \quad (2.6)$$

where $G_{\mu\nu} \equiv R_{\mu\nu} - \frac{1}{2}g_{\mu\nu}R$ is the Einstein tensor. It is a linear combination of the Ricci curvature tensor and scalar, which in turn are nonlinear, tensorial compositions of the Christoffel symbols and their derivatives:

$$R_{\mu\nu} = \Gamma_{\mu\nu,\sigma}^{\sigma} - \Gamma_{\mu\sigma,\nu}^{\sigma} + \Gamma_{\mu\nu}^{\sigma}\Gamma_{\sigma\lambda}^{\lambda} - \Gamma_{\mu\lambda}^{\sigma}\Gamma_{\nu\sigma}^{\lambda}$$

$$R = g^{\mu\nu} R_{\mu\nu}.$$

On the other side of the Einstein equations (2.6) is the matter tensor, the exact form and composition of which generally depends upon what is present—be it dust,

fluid, electromagnetic fields, scalar fields, vacuum, etc. Since we are using a massless scalar field, the stress-energy tensor—found by varying the matter Lagrangian with respect to the metric—is:

$$\begin{aligned} T_{\mu\nu} &= \frac{\delta\mathcal{L}_M}{\delta g^{\mu\nu}} \frac{1}{\sqrt{-g}} \\ &= \partial_\mu\phi \partial_\nu\phi - \frac{1}{2}g_{\mu\nu} \partial_\sigma\phi \partial^\sigma\phi. \end{aligned} \tag{2.7}$$

The matter tensor is multiplied in the equations by $\kappa = \frac{8\pi G_5}{c^4}$, G_5 being the five-dimensional version of Newton’s constant and c , of course, being the speed of light. Well might one ask how we are to know the strength of the gravitational coupling in five dimensions. Fortunately, the “actual” (SI) values of natural constants are of little concern in relativity, so we are free to *conveniently* adopt units wherein they are identically equal to unity—at the head-scratching cost of measuring mass, length, and time (and electric charge, were it to make an appearance) the same way. Thus we will use $\kappa = 8\pi$ from henceforth.

A priori, the scalar field and all components of the metric tensor are assumed to be functions of all the coordinates $(t, \rho, \theta, \varphi, \zeta)$, although we will shortly assert some helpful symmetries.

The equations may be manipulated into what will prove to be a more useful and convenient form by contracting both sides with the metric,² solving for R in terms of the contracted matter tensor T and inserting that result into the original:

$$R_{\mu\nu} = 8\pi \left(T_{\mu\nu} - \frac{1}{3}g_{\mu\nu}T \right). \tag{2.8}$$

If we insert the matter tensor (2.7) into these equations (2.8), they condense to

² This is done by a double inner-product with the metric; *e.g.*, the Ricci tensor $R_{\mu\nu} = g^{\lambda\sigma} R_{\lambda\mu\sigma\nu}$ is the *contraction* of the Riemann tensor.

the remarkably simple form,

$$R_{\mu\nu} = 8\pi \partial_\mu \phi \partial_\nu \phi. \quad (2.9)$$

The equation of motion for the matter is found by setting equal to zero the variation of \mathcal{L} with respect to the scalar field, $\frac{\delta \mathcal{L}}{\delta \phi} = 0$. Not too surprisingly, it turns out that the matter field itself extremizes the action by obeying the covariant wave equation,

$$\nabla_\mu \nabla^\mu \phi = 0. \quad (2.10)$$

2.2 Spherical and Other Symmetries

Even with the aid of a sophisticated computer, the Einstein equations are very unwieldy when dealt with in full. To help simplify matters, symmetries are often sought and introduced to the system. Formally, the mathematical device used to accomplish this is the Killing vector, which is not so lethal as it sounds.

Suppose we were to make an infinitesimal (or “point”) transformation, in a process reminiscent of the Taylor expansion: $x^\mu \mapsto \bar{x}^\mu(x^\nu) = x^\mu + \varepsilon \xi^\mu(x^\nu) + \mathcal{O}(\varepsilon^2)$. This represents the mapping of each point x^μ to a neighboring new point \bar{x}^μ along the direction determined by the vector field ξ^μ . Applying this transformation in the usual way (2.1) to the metric tensor (albeit in the infinitesimal limit) gives:

$$\begin{aligned} g_{\mu\nu}(\bar{x}) &= \bar{x}_{,\mu}^\alpha \bar{x}_{,\nu}^\beta g_{\alpha\beta}(\bar{x}) \\ &= \left(\delta_\mu^\alpha + \varepsilon \xi_{,\mu}^\alpha \right) \left(\delta_\nu^\beta + \varepsilon \xi_{,\nu}^\beta \right) g_{\alpha\beta}(x^\mu + \varepsilon \xi^\mu(x^\nu)) + \mathcal{O}(\varepsilon^2) \\ &= \left(\delta_\mu^\alpha + \varepsilon \xi_{,\mu}^\alpha \right) \left(\delta_\nu^\beta + \varepsilon \xi_{,\nu}^\beta \right) \left(g_{\alpha\beta}(x) + \varepsilon \xi^\lambda g_{\alpha\beta,\lambda} \right) + \mathcal{O}(\varepsilon^2) \\ \therefore g_{\mu\nu}(\bar{x}) &= g_{\mu\nu}(x) + \varepsilon \left(g_{\alpha\nu} \xi_{,\mu}^\alpha + g_{\mu\beta} \xi_{,\nu}^\beta + g_{\mu\nu,\lambda} \xi^\lambda \right) + \mathcal{O}(\varepsilon^2). \end{aligned} \quad (2.11)$$

If the spacetime is to be symmetric with respect to ξ^μ , then this transformation should leave the metric unchanged, such that $g_{\mu\nu}(\bar{x}) = g_{\mu\nu}(x)$. Therefore, the old

metric appears on both sides of (2.11) and cancels; the remainder must be made to equal zero (to first order). This requires that the first-order quantity in (2.11), which happens to equal the Lie derivative of the metric with respect to ξ^μ , be made to vanish. The resulting equation for our transformation vector ξ^μ is called “Killing’s equation”:

$$\mathbf{L}_\xi g_{\mu\nu} \equiv \xi^\sigma \partial_\sigma g_{\mu\nu} + g_{\mu\sigma} \partial_\nu \xi^\sigma + g_{\sigma\nu} \partial_\mu \xi^\sigma = 0. \quad (2.12)$$

Or equivalently, $\nabla_\mu \xi_\nu + \nabla_\nu \xi_\mu = 0$, by the miraculous properties of the metric and covariant differentiation (Eq. 2.4).

Killing’s equation (2.12) can be used either to explore the symmetry of a given metric by teasing out its Killing vectors, or to restrict a metric to having specific symmetries by using known Killing vectors. In our case we desire spherical symmetry, and we know from our studies of group theory and infinitesimal displacements that the Killing vectors which represent this symmetry are (in Cartesian coordinates) the three angular momentum generators, $[\xi^i, \xi^j] = \epsilon^{ijk} \xi^k$, where

$$\epsilon^{ijk} \equiv \begin{cases} 1 & , \text{ for even permutations of } 123 \\ -1 & , \text{ for odd permutations of } 123 \\ 0 & , \text{ otherwise} \end{cases}$$

is the Levi-Civita antisymmetric tensor. Let it be made clear that the bold Roman indices $\mathbf{i}, \mathbf{j}, \mathbf{k}$ label the Killing vectors themselves, not their individual components; for their components we will retain the usage of Greek letters as outlined in Table 1. (This is why we are not particular about “balancing” the superscripts and subscripts in the implied sum in the commutator equation above, as we usually are when covariant and contravariant components are afoot.) Using the angular momentum generators as Killing vectors, then, will tell us what our metric should look like, as well as its functional dependence.

Written using differential operators as the basis, and following a transformation to

coordinates befitting our ansatz (*i.e.*, coordinates on the sphere: $\{\theta, \varphi\}$), the Killing vectors take the more familiar form of partial derivatives with respect to the angular coordinates, because that happens to be exactly what they are! One of the three Killing vectors is rendered particularly simple: $\xi = \xi^\sigma \partial_\sigma = \partial_\varphi$. Written as bare components in this representation, $\xi^\sigma = (0, 0, 0, 0, 1)$. We shall examine this one in more depth.

We return, for a moment, to Cartesian coordinates, so that we can construct an intelligent ansatz-metric. In Cartesian coordinates, this azimuthal Killing vector ∂_φ takes the familiar form $\xi = -y \partial_x + x \partial_y$. (The reason for doing this will become clear when we discuss regularity issues in (§ 3.1.1).) For any symmetric second-rank covariant tensor $Q_{\mu\nu}$ the equation for the Lie derivative of this tensor along this vector is given (2.12) as

$$\xi^\lambda Q_{\mu\nu,\lambda} + \xi^\lambda{}_{,\mu} Q_{\lambda\nu} + \xi^\lambda{}_{,\nu} Q_{\lambda\mu} = 0.$$

Written out in full, this becomes fifteen(!) equations, to wit:

$$\begin{array}{llll} y Q_{xx,x} - x Q_{xx,y} & = & 2Q_{xy} & y Q_{ty,x} - x Q_{ty,y} & = & -Q_{tx} \\ y Q_{yy,x} - x Q_{yy,y} & = & -2Q_{xy} & y Q_{tz,x} - x Q_{tz,y} & = & 0 \\ y Q_{xy,x} - x Q_{xy,y} & = & Q_{yy} - Q_{xx} & y Q_{\zeta t,x} - x Q_{\zeta t,y} & = & 0 \\ y Q_{zz,x} - x Q_{zz,y} & = & 0 & y Q_{\zeta x,x} - x Q_{\zeta x,y} & = & Q_{\zeta y} \\ y Q_{zx,x} - x Q_{zx,y} & = & Q_{zy} & y Q_{\zeta y,x} - x Q_{\zeta y,y} & = & -Q_{\zeta x} \\ y Q_{zy,x} - x Q_{zy,y} & = & -Q_{zx} & y Q_{\zeta z,x} - x Q_{\zeta z,y} & = & 0 \\ y Q_{tt,x} - x Q_{tt,y} & = & 0 & y Q_{\zeta \zeta,x} - x Q_{\zeta \zeta,y} & = & 0 \\ y Q_{tx,x} - x Q_{tx,y} & = & Q_{ty} & & & \end{array}$$

The solution to these equations can be found in terms of fifteen independent regular functions:

$$\begin{array}{ll} Q_{zx} & = \quad x f_1 - y f_2 \\ Q_{zy} & = \quad y f_1 + x f_2 \\ Q_{tx} & = \quad x f_3 - y f_4 \\ Q_{ty} & = \quad y f_3 + x f_4 \\ Q_{\zeta x} & = \quad x f_5 - y f_6 \\ Q_{\zeta y} & = \quad y f_5 + x f_6 \\ Q_{xx} & = \quad f_7 - 2xy f_8 + y^2 f_9 \\ Q_{yy} & = \quad f_7 + 2xy f_8 + x^2 f_9 \end{array} \quad \begin{array}{ll} Q_{xy} & = \quad (x^2 - y^2) f_8 - xy f_9 \\ Q_{tt} & = \quad f_{10} \\ Q_{\zeta \zeta} & = \quad f_{11} \\ Q_{zz} & = \quad f_{12} \\ Q_{zt} & = \quad f_{13} \\ Q_{\zeta t} & = \quad f_{14} \\ Q_{\zeta z} & = \quad f_{15} \end{array}$$

where the $f_i = f_i(t, x^2 + y^2, z, \zeta) \forall i \in \{1 \dots 15\}$.

We now want to transform closer to the coordinates we would like to use. The azimuthal Killing vector has told us that the natural thing to do is to make a coordinate transformation from the rectilinear coordinates (t, x, y, z, ζ) to quasi-cylindrical coordinates $(t, \varrho, \varphi, z, \zeta)$. This coordinate transformation can be written as:

$$t = t; \quad x = \varrho \cos \varphi; \quad y = \varrho \sin \varphi; \quad z = z; \quad \zeta = \zeta;$$

so that the transformation matrix (2.1) is

$$\frac{\partial x_{rect.}^\mu}{\partial x_{cyl.}^\alpha} = \begin{bmatrix} 1 & 0 & 0 & 0 & 0 \\ 0 & \cos \varphi & -\varrho \sin \varphi & 0 & 0 \\ 0 & \sin \varphi & \varrho \cos \varphi & 0 & 0 \\ 0 & 0 & 0 & 1 & 0 \\ 0 & 0 & 0 & 0 & 1 \end{bmatrix} \quad (2.13)$$

Thus transforming the Cartesian components to cylindrical coordinates, and specifically equating this erstwhile generic tensor with the metric, $Q_{\mu\nu} = g_{\mu\nu}$, allows us to determine the structure and functional behavior of the full 5-metric. The transformation (2.10) tells us, somewhat miraculously, that

$$\begin{aligned} g_{\varrho\varrho} &= f_7 & , & & g_{\varphi\varphi} &= \varrho^2 f_7 + \varrho^4 f_9 & , & & g_{\zeta\zeta} &= f_{11} \\ g_{z\varrho} &= \varrho f_1 & , & & g_{tt} &= f_{10} & , & & g_{\zeta t} &= f_{14} \\ g_{z\varphi} &= \varrho^2 f_2 & , & & g_{tz} &= f_{13} & , & & g_{\zeta z} &= f_{15} \\ g_{\varrho\varphi} &= \varrho^3 f_8 & , & & g_{t\varrho} &= \varrho f_3 & , & & g_{\zeta\varrho} &= \varrho f_5 \\ g_{zz} &= f_{12} & , & & g_{t\varphi} &= \varrho^2 f_4 & , & & g_{\zeta\varphi} &= \varrho^2 f_6 \end{aligned}$$

We reiterate that the functions f_i are dependent on $t, \varrho^2 \equiv x^2 + y^2, z,$ and ζ . If we subsequently consider the other two Killing vectors in the set $\vec{x} \times \vec{\nabla}$, and likewise transform to spherical coordinates, we find our toy-universe is even more simplified. In particular, it may be shown that all metric functions ($g_{\varphi\varphi}$ being the only, and expected, exception), as well as all matter functions (if the generic $Q_{\mu\nu}$ is equated to the matter tensor $T_{\mu\nu}$) depend only upon the timelike coordinate, t , the spherical-

radial coordinate squared, $\rho^2 = \varrho^2 + z^2 = x^2 + y^2 + z^2$, and the orthogonal spacelike coordinate, ζ .

Simplified as this scenario is, we should also like, at this early stage, to keep the system invariant with respect to the extra coordinate, ζ . In this we depart from expecting any black strings to “bead up” into some hyperdimensional black pearl necklace as conjectured by Gregory and Laflamme [13]; rather they will appear to the hyperobserver more like black spaghetti. Nevertheless it is hoped that even with this enormous simplification interesting phenomenological effects of an inactive extra dimension might be observed in numerical simulation.

Mathematically, we implement our simplification by assuming, as an analytical fiat, the Killing vector $\xi = \xi^\alpha \partial_\alpha = \partial_\zeta$. Which is to say, in English: *Henceforth let ζ have no effect, only insofar as its presence necessitates the introduction of an extra term to the invariant interval.*

Significantly, when this Killing vector is applied together with the complete set of $SO(3)$ generators and a transformation is made to spherical coordinates, one may show in like manner to the preceding work that the functional dependence found in cylindrical coordinates persists, and even grows stronger:

$$\begin{array}{llll}
 g_{\rho\rho} & = & F_1 & , & g_{\theta\theta} & = & \rho^2 F_1 + \rho^4 F_2 & , & g_{\zeta\zeta} & = & F_3 \\
 g_{\rho\theta} & = & 0 & , & g_{\varphi\varphi} & = & g_{\theta\theta} \sin^2 \theta & , & g_{\zeta t} & = & 0 \\
 g_{\rho\varphi} & = & 0 & , & g_{\theta\varphi} & = & 0 & , & g_{tt} & = & F_5 \\
 g_{\rho\zeta} & = & \rho F_4 & , & g_{t\theta} & = & 0 & , & g_{\zeta\varrho} & = & 0 \\
 g_{\rho t} & = & \rho F_6 & , & g_{t\varphi} & = & 0 & , & g_{\zeta\varphi} & = & 0
 \end{array}$$

Here the F_i are the spherical analogues of the cylindrical f_i , *i.e.*, $F_i = F_i(t, \rho^2)$. Notice how the extra demands of spherical symmetry have reduced many components to zero. Furthermore, later on in our investigation the functional form of the remaining components becomes key to considerations of regularity at the origin.

To summarize the preceding, we have assumed symmetries with respect to all possible rotations, as well as translations in the extra dimension. These assumed

symmetries, put into force via Killing vectors, have revealed the structure of the metric and the functional form of its several components. We are left with sufficient coordinate freedom to make one of two possible gauge choices, as will be explored in the following chapter.

Chapter 3

Plan of Attack

3.1 Roads Not Taken

It is now necessary to carefully choose our plan of attack, as not all approaches to our problem are equally suited to the task. Our first order of business is to find the equations of motion using our symmetry assumptions and a set of coordinates which will give us a set of equations which are stable under finite differencing.

- *Schwarzschild method*

As an example, we could take our Killing-constructed, reasonable form for the 5-metric $g_{\mu\nu}$, and “plug-’n’-chug” to get the Einstein equations in the hopes that they would be analytically or numerically solvable.

This approach works perfectly in obtaining the static, spherically symmetric solutions of Schwarzschild and Reisser-Nördstrom. A clever coordinate maneuver can then introduce angular momentum a là Kerr.

However, blindly charging ahead in a *dynamical* relativity problem—even with a good, informed guess for the metric—yields a morass of PDEs in which the time derivatives (which are obviously essential to evolving the system) are irretrievably, nonlinearly mingled with other quantities. The reader is cordially invited to see for him- or herself how ugly it gets, or may just take our word for it.

- *S-wave method*

Because the direct frontal assault doesn’t pan out, we need something more clever.

Recall that when Killing's equation was used with spherical Killing vectors in Cartesian coordinates, and the results subsequently transformed to spherical-like coordinates, we came to believe that the metric components' functional form was

$$\begin{aligned} g_{\rho\rho} &= F_1(t, \rho^2) & , & & g_{\theta\theta} &= \rho^2 (F_1(t, \rho^2) + \rho^2 F_2(t, \rho^2)), \\ g_{\zeta\zeta} &= F_3(t, \rho^2) & , & & g_{\zeta\rho} &= \rho F_4(t, \rho^2), \end{aligned}$$

among other things. One possibility this form suggests is that we take $F_4 = 0$; $F_3 = F_1$ (so that the (ρ, ζ) plane is conformally flat); and that we combine $g_{\theta\theta}$ into one squared function of ρ^2 , $g_{\theta\theta} = s^2 = \rho^2 (F_1(t, \rho^2) + \rho^2 F_2(t, \rho^2))$. So doing allows us to “divide out” the spherical symmetry by separating the metric, cleaving it into two block-diagonal parts:

$$g_{\mu\nu} = \tilde{g}_{\mu\nu} + s^2 \sigma_{\mu\nu} = \tilde{g}_{ab} \delta_{\mu\nu}^{ab} + s^2 \sigma_{mn} \delta_{\mu\nu}^{mn},$$

enforcing our alphabetical convention (Table 1) with compound Kronecker deltas wherein each vertical pair of indices represents a separate identity matrix. The two-dimensional tensor $\sigma_{mn} = \text{diag}(1, \sin^2(\theta))$ is the metric of the unit two-sphere and \tilde{g}_{ab} is the metric of the remaining $2 + 1$ spacetime. The unknown function s^2 essentially measures gravitational distortion in “radial” distances; it could be interpreted geometrically as being related to the area of surfaces with constant t , ρ , and ζ , or of the spherical cross-sections of our black string.

From this metric the Christoffel symbols and Ricci curvature components can be generated (and those Kronecker deltas are a real lifesaver in that regard!). Upon doing so, one finds that

$${}^{(5)}R_{\mu\nu} = \begin{pmatrix} {}^{(3)}\tilde{R}_{ab} - \frac{2}{s} D_a D_b s & \mathbf{0}_{3 \times 2} \\ \mathbf{0}_{2 \times 3} & {}^{(2)}R_{mn} - \sigma_{mn} D_a (s D^a s) \end{pmatrix}. \quad (3.1)$$

In keeping with the notation set forth in Table 1, the Ricci curvature corresponding

to, and generated from, the reduced 3-metric \tilde{g}_{ab} has been labeled as ${}^{(3)}\tilde{R}_{ab}$. Likewise the Ricci curvature of the unit sphere with metric σ_{mn} is called ${}^{(2)}R_{mn}$; of note, σ_{mn} happens to be one of a small collection of “eigentensors” for the “Ricci-operator,” in the sense that ${}^{(2)}R_{mn} = \mathbf{R}(\sigma) \propto \sigma_{mn}$. In this case the proportionality constant is simply unity, so that

$${}^{(2)}R_{mn} = \sigma_{mn}. \quad (3.2)$$

Our manipulated Einstein equations (2.8) inform us that this Ricci tensor, ${}^{(5)}R_{\mu\nu}$, is proportional to the stress-energy tensor built from our scalar field; therefore,

$${}^{(3)}\tilde{R}_{ab} - \frac{2}{s}D_a D_b s = 8\pi \partial_a \phi \partial_b \phi \quad (3.3)$$

$${}^{(2)}R_{mn} - \sigma_{mn} D_a (s D^a s) = 8\pi \partial_m \phi \partial_n \phi. \quad (3.4)$$

Because $\partial_m \phi = 0$ (owing to our Killing vectors’ elimination of angular dependencies), the right-hand side of the second equation (3.4) must vanish. In addition, because of the relationship (3.2) between the angular Ricci components and the metric of \mathbf{S}^2 , the left hand side may be factored as a scalar quantity multiplying the two-metric. Since this must be true for all coordinate and field values, the scalar factor must also be equal to zero. After making these adjustments and algebraically re-arranging, the Einstein field equations take the form

$${}^{(3)}\tilde{R}_{ab} - \frac{2}{s}D_a D_b s = 8\pi \partial_a \phi \partial_b \phi \quad (3.5)$$

$$D_a (s D^a s) = 1 \quad (3.6)$$

When coupled with the equations of motion for the scalar field ϕ , these constitute the set of equations we should like to solve. This set of equations, as written, has an appealing interpretation, wherein s can be thought of as a scalar field unto itself,

propagating along with ϕ in the $2 + 1$ spacetime. With respect to the original $4 + 1$ manifold, s can be interpreted as a radiating gravitational degree of freedom.

There is a dire problem, however, with this formulation. As is well-known, any set of differential equations must be augmented by appropriate boundary conditions. Attractive as the s -wave interpretation is, the equation which s satisfies, due to regularity conditions on $g_{\theta\theta} = s^2$, must either (1) satisfy a very strange boundary condition for the putative wave, or else (2) be transformed into an equation bearing coordinate singularities that cannot be removed numerically (in any simple way). This latter problem is related to the fact that our nonlinear wave equation is not only inhomogeneous but has a constant source (3.6)—its solution, we found, is an endlessly-growing parabola. This fascinating but physically implausible situation will be discussed at greater length in (§ 3.2.2).

The larger problem with this formulation touches on our ultimate coordinate choices and the vital role regularity plays in numerical relativity. We shall complete our coordinate construction in the next chapter. However, having tried this false start gave us an opportunity to explore and better understand the regularity issues, which we will now present.

3.1.1 Regularity Issues

The s -wave equation (3.6) has something to teach us about the importance of regularity which is worth looking at in some detail. The equation, despite its appearance, fails to be the kind of wave equation with which we are familiar, because of boundary conditions which trace back to regularity. We would naturally expect that far from the scene of the collapsing scalar field ϕ , our system's spacetime would asymptotically approach flat, or Minkowski spacetime. Therefore, the radiating field s should resemble the radial coordinate ρ for $\rho \gg 0$, but we are hard-pressed to

consider as real a wave that grows in unbounded linearity at spatial infinity.

This behavior forces us to pause and consider the importance of regularity in tensor equations under the assumption of symmetries beyond mere translational. Clearly, we would prefer to model fields that exhibit *regular* behavior in the vicinity of fixed points of the symmetry (origin, axis, etc.). A simple manifestation of the potential problem is found in the cylindrically-symmetric Laplace equation in 2-D when written in polar coordinates (ϱ, ϑ) . This equation, for a generic scalar field ψ , is

$$\begin{aligned} 0 = \nabla^2 \psi &= \frac{1}{\varrho} \frac{\partial}{\partial \varrho} \left(\varrho \frac{\partial \psi}{\partial \varrho} \right) + \frac{1}{\varrho^2} \frac{\partial^2 \psi}{\partial \vartheta^2} \\ &= \frac{\partial^2 \psi}{\partial \varrho^2} + \frac{1}{\varrho} \frac{\partial \psi}{\partial \varrho} + \frac{1}{\varrho^2} \frac{\partial^2 \psi}{\partial \vartheta^2} \end{aligned} \tag{3.7}$$

For anyone accustomed to PDEs it is almost beyond mundane to notice that the radial part of this equation includes a factor of $1/\varrho$, suggesting a singularity at $\varrho = 0$. While completely unsurprising, this is a consequence of the choice of coordinates and not of any true, physical singularity. Indeed, when considered in the context of Einstein’s relativity, we might consider this a central tenet, namely, that the physics of any situation is well-defined and therefore impervious to the coordinates used to describe it. The statement “physics is well-defined” at $\varrho = 0$ finds mathematical expression in the observation that the relevant term in the Laplacian is well-behaved as ϱ approaches zero despite the appearance of its inverse.

Therefore, the troublesome factor of $1/\varrho$ in our Laplacian above may be traced back to the fact that the Jacobian of the transformation from Cartesian to polar coordinates is singular at the origin, the polar coordinate system itself being ill-defined at $\varrho = 0$. It is a singularity in the analytical geometry, not in the physics itself: writing Laplace’s equation in, say, Cartesian coordinates shows that the problem goes away.

The reason for our interest in this perhaps arcane distinction is that computers

don't know or care about whether a singularity is physical or mathematical, let alone how to deal with it.

In the Laplace equation, as $\varrho = 0$ is approached, the prefactor on the first-order derivative blows up; therefore, to maintain regularity the derivative must in fact vanish: $\psi_{,\varrho}|_{\varrho=0} = 0$. Thus the quantity $\lim_{\varrho \rightarrow 0} \frac{1}{\varrho} \frac{\partial \psi}{\partial \varrho}$ is finite.

At the continuum level this is perfectly reasonable and we accept it without further argument. However, the $\varrho \rightarrow 0$ limit implies that a delicately orchestrated cancellation of approximated quantities must occur in a discretized version of this equation. Numerically this can be exceedingly difficult to implement, but one is aided by a clear understanding of the behavior of various functions *i.e.*, tensor components, as these problem points in the coordinate system are approached ($\varrho = 0$ being the canonical example).

We saw hints of this in the discussion on Killing vectors, symmetry, and the functional dependence of quantities in our problem. To make progress with our code, we will use that understanding from symmetry as well as a variety of tricks in differencing terms such as that shown in the above Laplacian. The basic approach can be illustrated by how we might treat the above term. First, exactly as previously stated, we know from the continuum limit, that the derivative of ψ with respect to ϱ must vanish. As a result we know it vanishes and the total term must be finite at $\varrho = 0$. As a consequence, we can view ψ as an even function of ϱ (in the vicinity of $\varrho = 0$). With that in mind it becomes natural to difference this term with respect to ϱ^2 instead of ϱ . Doing this allows us to write

$$\frac{1}{\varrho} \frac{\partial \psi}{\partial \varrho} = 2 \frac{\partial \psi}{\partial (\varrho^2)} \tag{3.8}$$

by simple application of the chain rule. When differenced in this way, this term has

no obvious singular problems:

$$\left(\frac{1}{\varrho} \frac{\partial \psi}{\partial \varrho}\right)_n \approx 2 \frac{\psi_{n+1} - \psi_{n-1}}{(\varrho_{n+1})^2 - (\varrho_{n-1})^2}$$

This should be contrasted with a more naïve discretization such as

$$\left(\frac{1}{\varrho} \frac{\partial \psi}{\partial \varrho}\right)_n \approx \frac{1}{\rho_n} \frac{\psi_{n+1} - \psi_{n-1}}{\varrho_{n+1} - \varrho_{n-1}}.$$

In this second discretization, a problem arises in that the difference in ψ at two points as ρ approaches the origin must decrease like ρ so as to cancel the ρ in the denominator. While certainly possible, experience has shown that this is usually a delicate cancellation which is difficult to enforce. On the other hand, the first discretization requires no such cancellation, but rather exploits the known functional dependence (even-ness in ρ) found in the continuum limit.

Our hope is to make similar observations for more complicated tensor equations such as Einstein's, in which terms such as this persist after abandoning the s -wave approach.

Our approach now is to discover the functional behavior of tensor components in the vicinity of the origin when we assume spherical symmetry in our 5-D spacetime. Our assumption of regularity, then, will be as follows: we will assume that all tensor components, when written in a Cartesian basis, are regular functions of all the coordinates. Specifically, all these Cartesian tensor components are expandable in five-dimensional Taylor series everywhere regular. Once we have a functional form of the tensor components in a Cartesian basis, we will transform to coordinates better suited to our assumed symmetries. Naturally, the tensor transformation law (2.1), which we use to go from one coordinate system to another, mixes up various tensor

components in order to define the tensor components in this new basis:

$$\bar{T}_{ab} = \frac{\partial x^c}{\partial \bar{x}^a} \frac{\partial x^d}{\partial \bar{x}^b} T_{cd} \quad (2.1')$$

We can get the form of the tensor components in a Cartesian basis using our symmetries. Of course, we have already done this in (§ 2.2). There we saw the functional dependence of the components of \mathbf{Q} on (t, x, y, z, ζ) . Already in that section we transformed to a more convenient set of coordinates and found the behavior of those tensor components (now to be considered metric components) in the vicinity of the fixed point of our \mathbf{S}^2 . We saw in our previous exploration of Killing-enforced symmetries, for instance, that the component $g_{\rho\rho}$ is an even function of ρ and independent of ζ and the angular coordinates. Similarly, the component $g_{t\rho}$ was determined to be an odd function of ρ . Our intent is to exploit this understanding of the behavior of these components as ρ goes to zero, anticipating that there will be terms in our equations which involve quantities such as $\frac{1}{\rho}\partial_\rho g_{\rho\rho}$.

3.2 Sliced Spacetime: The Best Thing Since Sliced Bread

Whether or not we divide out the spherical symmetry, it is still imperative to sacrifice the equal footing which Einstein gave to temporal and spatial coordinates: for the sake of performing a dynamical evolution we *must* draw a distinction between time and space. As noted previously, blindly charging ahead, even with a sensible metric, comes at the cost of yielding horrendous equations that take a nontrivial number of pages just to write down.

To this end comes the technique developed by Arnowitt, Deser, and Misner (ADM) in 1962 [23]. In the discarded *s*-wave approach, we also eventually implemented this technique; the difference—and the genius—is in using the ADM decomposition on the full 5-dimensional problem rather than on a 3-D submanifold, with its manifest

s -related irregularities.

Conceptually this requires us to imagine spacetime foliated into myriad spatial “slices.” Each slice will represent the system at a particular moment in “time”—although what “time” means here will not necessarily be the same as what we usually think of as time. Spatial components on each slice will be indexed with Latin capitals per the specifications in Table 1.

Mathematically the ADM approach involves segregating the Einstein equations into two camps: those that govern the system’s evolution, and those that provide constraints that must be satisfied on each individual slice.

Math meets concept when one considers the relationship of a pair of points (P, Q) , one on each of two consecutive four-dimensional spatial slices. Let the point Q on the latter slice correspond to point P on the earlier slice. Presumably, in evolving into Q , point P may have “moved,” perhaps due to changes in the local curvature, or due to a coordinate change between slices.

We define the *lapse* function (α) as the change in proper time between two corresponding points in the two slices, and the *shift* vector field (β^A) measures their spatial displacement.

Furthermore, since we are in a sense removing ourselves to an outside perspective on all these slices, viewing them as being embedded in a larger space, we may define a unit normal, n^μ , to the spatial slices. Naturally a normal to spatial slices would be timelike, so $n^\mu n_\mu = -1$. One would expect, since it maps points from one slice to their respective futures, that n^μ will be composed of the lapse and shift:

$$n_\mu = (-\alpha, 0, 0, 0, 0); \tag{3.9}$$

$$n^\mu = \left(\frac{1}{\alpha}, -\frac{\beta^\rho}{\alpha}, \frac{\beta^\theta}{\alpha}, \frac{\beta^\varphi}{\alpha}, \frac{\beta^\zeta}{\alpha} \right). \tag{3.10}$$

(Note that these are different components of the selfsame unit normal timelike vector

\mathbf{n} ; the important role of basis-vectors as illustrated in Figs. 2.1, 2.2 now becomes much more real.) Our assumed symmetries cause all but one of the normal's spacelike components, namely the radial shift β^ρ , to be zero, such that $n^\mu = \left(\frac{1}{\alpha}, -\frac{\beta^\rho}{\alpha}, 0, 0, 0\right)$. Note also that we have made the shift explicitly negative, in anticipation of the expected collapse-behavior: point P should be shifted radially inward to become Q .

As in the s -wave approach, the metric of the $4 + 1$ spacetime is again broken into two parts. *Unlike* $\tilde{g}_{\mu\nu} + s^2\sigma_{\mu\nu}$, however, this partitioning of the metric is actually useful:

$$g_{\mu\nu} = \gamma_{\mu\nu} - n_\mu n_\nu. \quad (3.11)$$

Strictly speaking, the spatial slice metric $\gamma_{\mu\nu}$ can and does have a nonzero tt -component. Accordingly, we will use γ_{AB} , with Latin uppercase indices, to denote the metric of the slices (see Table 1). The invariant interval, therefore, in a sliced-spacetime scheme, is given as

$$\begin{aligned} ds^2 &= -\alpha^2 dt^2 + \gamma_{AB}(dx^A + \beta^A dt)(dx^B + \beta^B dt) \\ &= (-\alpha^2 + \gamma_{AB}\beta^A\beta^B)dt^2 + 2\beta^A\gamma_{AB} dt dx^B + \gamma_{AB}dx^A dx^B. \end{aligned} \quad (3.12)$$

Rearranging (Eq. 3.11), we obtain the projection operator: $\gamma_\mu^\nu = \delta_\mu^\nu + n_\mu n^\nu$; that is, γ_μ^ν projects 5-D quantities onto the purely spatial slices.

Since the spatial slices are manifestly submanifolds embedded in our complete spacetime, we would do well to consider the slices' geometry from the perspective of the full 5-D universe. Each embedded slice is or can be bent and distorted; the most straightforward means of describing the distortion would be the "outer derivative" of the normal, projected onto the slice itself. Therefore, we define the extrinsic curvature as

$$K_{AB} = - \perp \nabla_A n_B, \quad (3.13)$$

in which “ \perp ” is shorthand for “the projection operator ($\perp_B^\mu \equiv \gamma_B^\mu$) has been applied to every free index.” The extrinsic curvature is symmetric ($K_{AB} = K_{BA}$) and is orthogonal to n^μ with respect to either index. Hence it is a spatial quantity that lives wholly in the hypersurface, or slice. The extrinsic curvature thus defined will become an important variable in the equations that govern the behavior of our system.

3.2.1 The ADM Strategy

The ADM equations, which express the Einstein equations in terms of time derivatives of the metric and the extrinsic curvature of the spatial slices, are given as follows:

$$\partial_t \gamma_{AB} = \Delta_A \beta_B + \Delta_B \beta_A - 2\alpha K_{AB}; \quad (3.14)$$

$$\begin{aligned} \partial_t K_{AB} = & \beta^C \Delta_C K_{AB} + K_{AC} \Delta_B \beta^C + K_{BC} \Delta_A \beta^C - 2\alpha K_{AC} K_B^C \\ & - \Delta_A \Delta_B \alpha + \alpha \left(K K_{AB} + {}^{(4)}\mathcal{R}_{AB} - \perp {}^{(5)}R_{AB} \right). \end{aligned} \quad (3.15)$$

These hyperbolic equations are supplemented by elliptical constraint equations derived from purely geometrical relations which are true for any $N - 1$ dimensional spacelike foliation of any N -dimensional manifold.

To obtain these equations one begins by projecting the full N -dimensional Riemann tensor onto the slice ($\perp R_{ABCD}$) and contracting it with an arbitrary vector v^A tangent to the slice. After some indicial manipulations, and recognizing the Riemann tensor as the commutator of covariant differential operators, we have

$$v^A \perp R_{ABCD} = \perp (\nabla_D \nabla_C v_B - \nabla_C \nabla_D v_B). \quad (3.16)$$

Applying the projection operator to each index, as described in §3.2, and following more clever maneuvers, we arrive at the first of the famous Gauss-Codazzi (GC) relations:

$$\perp R_{ABCD} = \mathcal{R}_{ABCD} + K_{DB} K_{CA} - K_{CB} K_{DA}. \quad (3.17)$$

For generality's sake I have declined here to label the R 's with presuperscripts denoting dimension in order to emphasize the geometric generality. The calligraphic \mathcal{R} is the Riemann curvature of the generic $N - 1$ slice, and K is its extrinsic curvature, as defined previously (3.12).

Upon contracting both sides with the full metric in the pairs $\{BD\}$ and $\{AC\}$, we get the so-called ‘‘Hamiltonian’’ or energy constraint:

$$\begin{aligned} {}^{(4)}\mathcal{R} - K_A^B K_B^A + K^2 &= {}^{(5)}R + 2 {}^{(5)}R_{\hat{n}\hat{n}} \\ &= {}^{(5)}R + 2 {}^{(5)}R_{\mu\nu} n^\mu n^\nu. \end{aligned} \quad (3.18)$$

Here at last we specify dimensions pertinent to our problem for future clarity. The reason it is called the energy constraint is the crucial role the timelike normal n^μ plays on the right hand side. Recall that we said that n^μ maps points on each slice to their respective future selves; *i.e.*, n^μ is like a generator of displacements in time—and so has at least an heuristic association with the Hamiltonian in quantum mechanics and in the Poisson formulation of classical mechanics.

Similar analysis, using an arbitrary normal n^μ (it keeps its full-manifold index as it is not confined to the slice) in place of the tangential vector used in the foregoing, gives the second GC relation,

$$\perp R_{ABC\hat{n}} \equiv \perp R_{ABC\mu} n^\mu = \Delta_B K_{AC} - \Delta_A K_{BC}, \quad (3.19)$$

which becomes, by similar metric contraction, another constraint:

$$\begin{aligned} \Delta_A K_B^A - \Delta_B K &= -\perp {}^{(5)}R_{B\hat{n}} \\ &= -{}^{(5)}R_{\mu\nu} \gamma_B^\mu n^\nu. \end{aligned} \quad (3.20)$$

We can also see in this equation a similar hint as to why it is sometimes called the ‘‘momentum’’ constraint: the projection operator γ_B^μ can be seen as telling us how far

things move along the slice, so is associated with a generator of translation—hence the connection with momentum.

The appearance of terms relating to the five-dimensional Ricci curvature on the right-hand side of the ADM and constraint equations suggests that we use the relativistic relation between curvature and matter to replace the ${}^{(5)}R$ terms with their scalar field equivalent, courtesy of Einstein’s equations.

With our symmetries in place and the ADM equations waiting in the wings, we are left with the relatively simple matter of making a final coordinate choice for the slice itself—one that will know only physical singularities and not cause problems at any coordinate singularities that may arise (such as an event horizon)—and from thence building the pieces that go into these equations.

3.2.2 Isotropic Coordinates and a Conformal Slice

Recall that the basic Schwarzschild solution, in standard 4-D spherical (or “Schwarzschild”) coordinates, is

$$ds^2 = - \left(1 - \frac{2m}{r}\right) dt^2 + \left(1 - \frac{2m}{r}\right)^{-1} dr^2 + r^2(d\theta^2 + \sin^2 \theta d\varphi^2).$$

It contains a coordinate singularity at the so-called event horizon, $r = 2m$, as well as the physical singularity at the origin. While this gives rise to fascinating investigations into black hole event horizons, ‘tis hardly conducive to computer simulations, where any singularity is a *bad* singularity—particularly one beyond which space and time seemingly switch roles.

It is therefore sometimes useful to consider a change to “isotropic” coordinates such that our $t = \text{constant}$ slices will be “as close as we can get them to Euclidean 3-space” [30] which has no particular issue with the sphere $r = 2m$.

The transformation desired turns out to be $r = \rho \left(1 + \frac{m}{2\rho}\right)^2$, in which case the

Schwarzschild metric takes the isotropic form

$$ds^2 = - \left(\frac{1 - \frac{m}{2\rho}}{1 + \frac{m}{2\rho}} \right)^2 dt^2 + \left(1 + \frac{m}{2\rho} \right)^4 (d\rho^2 + \rho^2(d\theta^2 + \sin^2 \theta d\varphi^2)); \quad (3.21)$$

note that the erstwhile coordinate singularity at $r = 2m$, which corresponds to $\rho = m/2$, has disappeared in the new coordinates, as desired. The function multiplying the spatial terms is called the *conformal* factor, because angles and ratios of length (within the spatial slice) are preserved regardless of its value.

This example shows the pattern we can follow in setting up a five-dimensional metric for our problem

So, in compiling our metric we would like to use (1) a conformal factor, (2) the lapse and shift of ADM, and (3) our understanding of regularity conditions from (§ 3.1.1). In particular, we can see from our discussion of regularity that in general before making a spatial coordinate choice the spatial metric must take the form

$$d\ell^2 = d\rho^2 F_1 + 2\rho d\rho d\zeta F_4 + d\zeta^2 F_3 + (\rho^2 F_1 + \rho^4 F_2)(d\theta^2 + \sin^2 \theta d\varphi^2)$$

where all the F_i are functions of t and ρ^2 only. Choosing spatial coordinates boils down to finding relationships between these arbitrary¹ functions F_i . As we have seen, one possible choice is $F_4 = 0$, $F_1 = F_3$, which creates the aforementioned “scalar field” $s^2 = \rho^2(F_1 + \rho^2 F_2)$. This elaborates on our earlier point, that s has to go like ρ . With this formulation, one can see that doing the decomposition suggested earlier leaves us with a quantity satisfying a constant-sourced wave equation (3.6) but having boundary conditions that diverge at infinity.

To see what we mean about this nasty boundary condition, consider what the F_i have to do at infinity in order for the metric to “match up” to flat space, or

¹ Not entirely arbitrary; the F_i must, of course, satisfy the Einstein equations.

$d\ell^2 = d\rho^2 + \rho^2(d\theta^2 + \sin^2\theta d\varphi^2) + d\zeta^2$. F_2 must vanish, and F_1 must go to unity (or at least to some positive constant that may be rescaled to unity). However, this forces s to literally go as ρ all the way to infinity. From the perspective of the wave equation, this is a recipe for disaster.

An alternative is to divide out the divergent behavior of s by setting $s = \rho e^\varsigma$, thus placing the expected divergent behavior in the factor of ρ and making ς the scalar field one watches evolve (in hopes that ς will prove itself well-behaved). To that end, we would like to get the s -wave equation (3.6) into the classic wave-equation form for γ itself, $\square^2\varsigma = H(\rho, \varsigma)$.

Upon substituting $s = \rho e^\varsigma$, our pesky wave equation, $D_a(s D^a s) = 1$ becomes

$$D_a D^a(\rho e^\varsigma) = \frac{1 - D_a(\rho e^\varsigma) D^a(\rho e^\varsigma)}{\rho e^\varsigma}$$

The simple exercise of expanding the derivatives of ρe^ς will be left to the interested reader. Upon those expansions and some algebraic rearrangement, the metric-wave equation becomes

$$\partial_a \partial^a \varsigma = \frac{e^{-2\varsigma} - \tilde{g}^{\rho\rho}}{\rho^2} - \frac{4\partial^\rho \varsigma}{\rho} - 2\partial_a \varsigma \partial^a \varsigma \quad (3.22)$$

The big problem with equation (3.22) is the first term. The numerator must go as ρ^2 , to avoid ugly behavior at infinity and at the origin. This is fine and dandy in the continuum limit, but there are no tricks to enforce it numerically, or to make it go away (as absorbing unwanted factors of ρ into a derivative operator).

Therefore, try as we might, we could not get a stable evolution out of this setup. Suffice it to say, taking this tack leads the unwary investigator down a long, dark, and loathsome path, until he is hopelessly bogged down in a swamp of intractable singularities and equations that bear not the slightest resemblance to the sexy Einstein equations they once were.

The alternative, which we danced around until stumbling upon it, was a different gauge choice, namely to set $F_4 = F_2 = 0$. This leaves the ρ - θ - φ sector of the metric conformally flat, with a conformal factor of F_1 , which henceforth shall be called ψ^4 . Meanwhile, F_3 may, without loss of generality, be set equal to $F_1 \bar{F}_3 = \psi^4 e^{2\sigma}$.

Under this construction, our invariant interval (3.13) will take the explicit form

$$ds^2 = \left(-\alpha^2 + \psi^4 \beta^{\rho^2}\right) dt^2 + 2\psi^4 \beta^\rho d\rho dt + \psi^4 \left(d\rho^2 + \rho^2 d\Omega^2 + e^{2\sigma} d\zeta^2\right) \quad (3.23)$$

$$= -\alpha^2 dt^2 + \psi^4 \left[(d\rho + \beta^\rho dt)^2 + \rho^2(d\theta^2 + \sin^2 \theta d\varphi^2) + e^{2\sigma} d\zeta^2\right]. \quad (3.24)$$

Here we see the recently introduced functions: $e^{2\sigma}$ is the metric component unique to ζ which we ever so briefly called \bar{F}_3 , and ψ is our yet-to-be-determined conformal factor. The presence of a $\sigma \neq -\infty$ keeps our coordinate system from being strictly isotropic, but that cannot and should not be helped, since we would like to see *some* dynamical effect from the extra dimension. Note also that, owing to our chosen Killing vectors (∂_ζ and the angular momentum generators ξ^i), the shift vector β^A has but one nonzero component (β^ρ).

A comment or two on the metric as presented above may help one's intuitive understanding of, and appreciation for, what it tells us.

The first casting (3.23) highlights the fact that we have chosen a conformal spatial slice and separates out the terms relating to the measure of time. In the second casting (3.24), the roles of α and β are more explicit: α as a kind of temporal scaling that depends on where and when you are; β looks very much the “shift” vector as it calls to mind the momentum vector \vec{k} in the argument $\omega t + \vec{k} \cdot \vec{r}$ for an infalling wave.

Notice also that rotating black hole solutions are often cast in a form similar in spirit to (3.24), with $(A d\phi + B dt)^2$'s showing up to emphasize the fact that time is intimately tied up with azimuthal angle, time itself being dragged along with

the rotation, especially within the ergosphere. So the form we see makes sense: we'd expect, in a spherically symmetric collapse, to see time being dragged into the prospective black hole in the radial direction.

Chapter 4

Molding the Equations Like Wet Clay

4.1 Non-zero Components of the Slice's Ricci Curvature

Utilizing *MAPLE 9.5*'s built-in tensor package, it is short work to obtain the following components of ${}^{(4)}\mathcal{R}_{AB}$ (after some decidedly non-*MAPLE*-ish aesthetic re-arrangement):

$${}^{(4)}\mathcal{R}_{\rho\rho} = - \left[\sigma'' + \sigma'^2 + \frac{2\psi'}{\psi} \left(\sigma' + \frac{2}{\rho} \right) + 6 \left(\frac{\psi'}{\psi} \right)' \right]; \quad (4.1)$$

$${}^{(4)}\mathcal{R}_{\theta\theta} = -\rho^2 \left[\frac{8(\rho\psi')'}{\rho\psi} + \sigma' \left(\frac{2\rho\psi' + \psi}{\rho\psi} \right) + 6 \left(\frac{\psi'}{\psi} \right)' \right]; \quad (4.2)$$

$${}^{(4)}\mathcal{R}_{\varphi\varphi} = {}^{(4)}\mathcal{R}_{\theta\theta} \sin^2 \theta; \quad (4.3)$$

$${}^{(4)}\mathcal{R}_{\zeta\zeta} = -e^{2\sigma} \left[\sigma'' + \frac{2\sigma'}{\rho} + \sigma'^2 + \frac{2(\rho^2\psi')'}{\rho^2\psi} + \frac{6\psi'}{\psi} \left(\sigma' + \frac{\psi'}{\psi} \right) \right]. \quad (4.4)$$

(Primes denote partial differentiation with respect to ρ ; we shall also be using overdots to denote partial time derivatives. Also, by way of full disclosure I should note that *MAPLE* contracts on a different pair of Riemann indices in producing the Ricci tensor, necessitating the forced introduction of a negative sign in order to have agreement with work done by hand, including the derivation of crucial ADM equations.)

As the Hamiltonian constraint requires the 4-D Ricci scalar, we must also calculate it;

$${}^{(4)}\mathcal{R} = \gamma^{AB} {}^{(4)}\mathcal{R}_{AB} = -\frac{2}{\psi^4} \left[\sigma'' + \frac{2\sigma'}{\rho} + \sigma'^2 \right] - \frac{12}{\psi^5} \left[\psi'' + \psi' \left(\frac{(\rho\psi)'}{\rho\psi} + \frac{\rho\sigma' + 1}{\rho} \right) \right]. \quad (4.5)$$

4.2 Constraints on α , \tilde{K}_ρ^ρ , and ψ

We first consider the equations of constraint, which must be satisfied on every time-slice of the evolution. In the process of so doing, we shall introduce new coordinate assumptions and new fields.

4.2.1 The Maximal Slicing Condition and a Constraint on α

General relativity’s coordinate invariance proves a mixed blessing—it introduces some strange ancillary fields, but also provides freedom to choose and change coordinate systems that avoid serious problems encountered along the way.¹

One such thing we shall do is rescale all components of K_A^B by the conformal factor, to wit: $\psi^2 K_A^B = \tilde{K}_A^B$. This we do in anticipation that a conformal extrinsic curvature will make certain equations (namely, the Hamiltonian), more easily dealt with.

Secondly, as our spacetime collapses into a black hole (as we hope it does), we may exploit the coordinate freedom of general relativity to select our spatial slices in such a way that they—and therefore neither the computer doing the calculation—never actually see the black hole’s singularity. Rather, the slices “pile up” and wrap forward as the singularity is approached. Intuitively this makes good sense, as we expect time to slow to a crawl near the black hole, but to march on as usual at points spatially

¹ One of the items on the tongue-in-cheek “Physicists’ Bill of Rights” is *the right to bring coordinate systems and frames of reference into existence at will*.

far removed from the scene of the collapse.

The spatial slices that do this can be shown to be those of the greatest volume; hence the method employing them is often called “*maximal slicing*.” Mathematically maximal slicing translates to setting the trace of the extrinsic curvature to zero: ${}^{(4)}K = K_\rho^\rho + K_\zeta^\zeta + K_\theta^\theta + K_\varphi^\varphi = 0$. This is of course also true of ${}^{(4)}\tilde{K}$.

The maximal slicing condition will allow us to simplify our equations, and indeed, to create a constraint that one would not expect to find: strange as it seems, the ADM equation describing how the extrinsic curvature evolves in time can actually be massaged into a static constraint equation.

First, we will need to raise one index of the evolving K_{AB} using the slice metric. Unfortunately this involves getting the metric through the time-differential operator, so it comes at the cost of picking up an extra term from the product rule:

$$\partial_t K_A^B = \partial_t(\gamma^{BC} K_{AC}) = \partial_t \gamma^{BC} K_{AC} + \gamma^{BC} \partial_t K_{AC}.$$

Now, a time derivative of the covariant slice metric, we could handle. The ADM equations, however, tell us naught about the contravariant slice metric. Fortunately it can be easily shown that $\dot{\gamma}^{BC} = -\gamma^{BE}\gamma^{CF}\dot{\gamma}_{EF}$.

$$\therefore \partial_t K_A^B = -\gamma^{BE}\gamma^{CF}\partial_t \gamma_{EF} K_{AC} + \gamma^{BC} \partial_t K_{AC}.$$

Into this we substitute our standard ADM evolution equations (3.14, 3.15) and contract on A and B . When the dust settles on that operation, we are left with the sublimely elegant statement,

$$\Delta^A \Delta_A \alpha = \alpha \left({}^{(4)}\mathcal{R} - {}^{(5)}R^* \right), \tag{4.6}$$

wherein our maximal slicing condition has permitted us to eliminate the derivative of $K_A^A = K$ and where the asterisk on the ${}^{(5)}R$ reminds us that it is the contraction of the *projected* 5-D Ricci curvature.

Upon substituting the $\partial \pm \Gamma$ expansion of the covariant derivatives and the appropriate Ricci scalars (slice for the first, matter for the second) into this equation and simplifying, we obtain

$$\alpha'' + \left(\sigma' + \frac{2}{\rho} + \frac{4\psi'}{\psi} \right) \alpha' + 2 \left[\sigma'' + \frac{2\sigma'}{\rho} + \sigma'^2 + 12 \left(\frac{\psi''}{\psi} + \frac{\psi'}{\psi} \left(\sigma' + \frac{2}{\rho} + \frac{\psi'}{\psi} \right) \right) + 4\pi\Phi^2 \right] \alpha = 0; \quad (4.7)$$

we have here introduced $\Phi = \partial_\rho \phi = \phi'$.

It is a never-ending source of wonder to us that the *evolution* equation for K_{AB} should lead to the *constraint* equation for α . Such is the miracle of maximal slicing. (One may wonder why we choose to treat this as “ α ’s” equation instead of, say, that of ψ or σ . The reason is simply that this equation, for all its apparent ugliness, is at least *linear* in one of its functions— α —thus lending itself to an eventual “tri-diag” numerical solution for α . Also, we will encounter other equations that can take care of ψ and σ .)

4.2.2 Introducing Ω , and a Constraint on \tilde{K}_ρ^ρ

The Killing vectors we chose are far-reaching in their effects. Recall that we derived the structure and functional form for any second rank, symmetric tensor $Q_{\mu\nu}$ —those rules apply as well to the extrinsic curvature tensor as to the metric and stress-energy tensors. In particular, this means that we require (after raising one of the indices in the usual way)

$$\tilde{K}_\rho^\rho = h_1(t, \rho^2); \quad \tilde{K}_\theta^\theta = \tilde{K}_\varphi^\varphi = h_1(t, \rho^2) + \rho^2 h_2(t, \rho^2); \quad \tilde{K}_\zeta^\zeta = h_3(t, \rho^2);$$

The gauge choice dismissed previously (s) had a field we called χ , which happened to be equal to the angular extrinsic curvature components. In that case $\tilde{K}_\rho^\rho + \tilde{K}_\zeta^\zeta =$

$h_1 + h_3$ was compressed into the single unknown K , with $h_2 = 0$ and $h_1 = \chi$. The maximal slicing condition then eliminated remaining ambiguity in saying that $2\chi + K = 0$. However, as we have seen, this is not a prudent course.

In our present approach the only viable option left, and therefore the natural choice, is to introduce $\rho h_2 = \Omega \equiv \frac{\tilde{K}_\theta^\theta - \tilde{K}_\rho^\rho}{\rho}$; $\tilde{K}_\zeta^\zeta = h_3$ will be determined by the maximal slicing condition. Note that Ω will be an odd function of ρ .

Between this “ Ω ,” the maximal slicing condition, and the conformal extrinsic curvature \tilde{K}_ρ^ρ , we can make substitutions whenever the following henceforth offending quantities appear:

$$\tilde{K}_\theta^\theta = \tilde{K}_\rho^\rho + \rho\Omega; \tag{4.8}$$

$$\tilde{K}_\zeta^\zeta = -(3\tilde{K}_\rho^\rho + 2\rho\Omega); \tag{4.9}$$

$$K_\rho^\rho = \frac{\tilde{K}_\rho^\rho}{\psi^2}; \tag{4.10}$$

$$K_\rho^{\rho'} = \frac{\tilde{K}_\rho^{\rho'}}{\psi^2} - \frac{2\psi'}{\psi^2}\tilde{K}_\rho^\rho. \tag{4.11}$$

This will have the effect of constraining our system to consider only \tilde{K}_ρ^ρ and Ω (h_1 and ρh_2).

Now, then, the momentum constraint (3.20) as established in chapter 3, is

$$\Delta_B K_A^B - \Delta_A K = -{}^{(5)}R_{\mu\nu} \gamma_A^\mu n^\nu.$$

It is first order in K , so we expect a first-order ODE for the curvature as a reward for our labors on this equation.

One may immediately see that the second term on the LHS vanishes by virtue of our maximal slicing condition.

Into the RHS, following the strategy outlined previously, we substitute the 5-D Einstein equation for the 5-D Ricci curvature and perform the specified contraction and projection:

$$\Delta_B K_A^B = -\frac{8\pi \partial_A \phi \Pi}{\psi^2}.$$

Using the Christoffel symbols provided by *MAPLE 9.5* to perform the covariant divergence, it becomes apparent that, because of the diagonality of K_A^B , the only nontrivial equation is that of ρ . Upon invoking the substitutions (4.8-11), we obtain the object of our momentary desires:

$$\tilde{K}_\rho^{\rho'} + \tilde{K}_\rho^\rho \left(\frac{6\psi'}{\psi} + 4\sigma' \right) + 2\Omega(\rho\sigma' - 1) + 8\pi\Phi\Pi = 0. \quad (4.12)$$

4.2.3 Introducing Π , and a Constraint on ψ

The Hamiltonian constraint (3.18),

$${}^{(4)}\mathcal{R} - K_A^B K_B^A + K^2 = {}^{(5)}R + 2{}^{(5)}R_{\mu\nu} n^\mu n^\nu,$$

is likewise nowhere near as challenging as it appears at first blush.

The RHS involves contractions of the 5-D Ricci tensor. We require the 5-D Ricci scalar and the projection normal to the slices:

$$\begin{aligned} {}^{(5)}R + 2{}^{(5)}R_{\mu\nu} n^\mu n^\nu &= g^{\mu\nu} {}^{(5)}R_{\mu\nu} + 2{}^{(5)}R_{\mu\nu} n^\mu n^\nu \\ &= 8\pi (g^{\mu\nu} + 2n^\mu n^\nu) \nabla_\mu \nabla_\nu \phi \\ &= \frac{8\pi}{\psi^4} (\Phi^2 + \Pi^2), \end{aligned} \quad (4.13)$$

where we have introduced the character $\Pi \equiv \psi^2 n^\mu \partial_\mu \phi$. We shall say more about Π later on.

Meanwhile, we must flesh out the left-hand side. The maximal slicing condition helps us by again forcing the final term to vanish. The first term we have already obtained (4.5), and $K_A^B K_B^A$ may be written as

$$K_A^B K_B^A = \sum_A (K_A^A)^2 = K_\rho^{\rho^2} + 2K_\theta^{\theta^2} + K_\zeta^{\zeta^2},$$

because K_A^B is diagonal, and because (as we have seen) $K_\theta^\theta = K_\varphi^\varphi$ by virtue of spherical symmetry. This of course may be further “simplified” by the substitutions (4.8-11):

$$K_A^B K_B^A = \frac{1}{\psi^4} (12\tilde{K}_\rho^{\rho^2} + 16\rho\Omega\tilde{K}_\rho^\rho + 6\rho^2\Omega^2).$$

After assembling all the pieces of the Hamiltonian constraint and prettying it up, we come to

$$\begin{aligned} \frac{\psi''}{\psi} + \frac{\psi'}{\psi} \left[\frac{2}{\rho} + \sigma' + \frac{\psi'}{\psi} \right] + \tilde{K}_\rho^{\rho^2} + \frac{4}{3}\rho\Omega\tilde{K}_\rho^\rho + \frac{1}{2}\rho^2\Omega^2 \\ + \frac{1}{6} \left(\sigma'' + \frac{2\sigma'}{\rho} + \sigma'^2 \right) + \frac{2}{3}\pi(\Phi^2 + \Pi^2) = 0 \end{aligned} \quad (4.14)$$

Equation (4.14) can in turn be used to render the α equation (4.7) simpler:

$$\alpha'' + \alpha' \left(\sigma' + \frac{2}{\rho} + \frac{4\psi'}{\psi} \right) - \alpha (6\rho^2\Omega^2 + 16\rho\Omega\tilde{K}_\rho^\rho + 12\tilde{K}_\rho^{\rho^2} + 8\pi\Pi^2) = 0. \quad (4.15)$$

4.3 Evolution equations

4.3.1 Evolution of Metric Fields

We now turn our attention to the dynamical equations for metric quantities. Obtaining these is done by a fairly straightforward application of the ADM equations. Recall that (3.14)

$$\partial_t \gamma_{AB} = \Delta_A \beta_B + \Delta_B \beta_A - 2\alpha K_{AB}.$$

Now, in this the index on $\vec{\beta}$ is covariant, whereas it is given to us as a contravariant vector. Also, the extrinsic curvature is double-covariant, whereas our preferred form is mixed type. Fortunately both of these issues are easily dealt with:

$$\begin{aligned} \partial_t \gamma_{AB} &= \Delta_A \beta_B + \Delta_B \beta_A - 2\alpha K_{AB} \\ &= \gamma_{BC} \Delta_A \beta^C + \gamma_{AC} \Delta_B \beta^C - 2\alpha \gamma_{BC} K_A^C \\ &= \gamma_{BC} \left(\Delta_A \beta^C - 2\alpha K_A^C \right) + \gamma_{AC} \Delta_B \beta^C \\ &= \gamma_{BC} \left(\partial_A \beta^C - 2\alpha K_A^C \right) + \gamma_{AC} \partial_B \beta^C + \beta^D \left(\gamma_{BC} \Gamma_{AD}^C + \gamma_{AC} \Gamma_{BD}^C \right) \end{aligned}$$

The combination of metrics and Christoffel symbols in the last term happens to equal $\gamma_{AB,D}$;

$$\begin{aligned} \therefore \quad \partial_t \gamma_{AB} &= \gamma_{BC} \left(\partial_A \beta^C - 2\alpha K_A^C \right) + \gamma_{AC} \partial_B \beta^C + \beta^D \partial_D \gamma_{AB} \\ &= \gamma_{B\rho} \partial_A \beta^\rho - 2\alpha \gamma_{BC} K_A^C + \gamma_{A\rho} \partial_B \beta^\rho + \beta^\rho \partial_\rho \gamma_{AB}, \end{aligned}$$

where we have performed the specified sums involving $\vec{\beta}$ and invoked the fact that $\beta^A = (\beta^\rho, 0, 0, 0)$. Now all that remains is to extract the explicit equations for each metric component. The evolutions of $\gamma_{\rho\rho}$ and $\gamma_{\theta\theta} = \gamma_{\varphi\varphi} \csc^2 \theta$ both give equations for $\dot{\psi}$:

$$\dot{\psi} = \beta^\rho \psi' + \frac{1}{2} \left(\beta^{\rho'} - \frac{\alpha \tilde{K}_\rho^\rho}{\psi^2} \right) \psi; \quad (4.16)$$

$$\dot{\psi} = \beta^\rho \psi' + \frac{1}{2\rho} \left(\beta^\rho - \frac{\rho \alpha \tilde{K}_\theta^\theta}{\psi^2} \right) \psi. \quad (4.17)$$

So, we have two equations for $\dot{\psi}$, and each should be true. In the coding we only use one of them (4.16), but for now we may set their corresponding right hand sides equal to each other; thus pops out one last, unexpected constraint equation, for β^ρ :

$$\beta^{\rho'} = \frac{\beta^\rho}{\rho} - \frac{\alpha \rho \Omega}{\psi^2}. \quad (4.18)$$

The ADM metric equations harbor one more component's evolution to find from the ADM equation, and that is σ 's:

$$\dot{\sigma} = \beta \sigma' - \beta^{\rho'} + \frac{\alpha}{\psi^2} \left(4\tilde{K}_\rho^\rho + 2\rho \Omega \right). \quad (4.19)$$

(Here we have used the first $\dot{\psi}$ equation to replace the term arising from the product rule in the time derivative; that is whence the \tilde{K}_ρ^ρ and $\beta^{\rho'}$ come. We could use (4.18) to replace the $\beta^{\rho'}$ in (4.19), but keeping the derivative is less painful than having a ρ^{-1} in the equations, so we won't worry about it.)

One equation thus far is conspicuously absent, and it is not surprising that it is from the ADM equation concerning the evolution of extrinsic curvature that we obtain the evolution of Ω , it being composed of extrinsic curvature components. The derivation, however, is long and unwieldy² and requires the use of *MAPLE* unless one wishes to go absolutely mad.

² Just *look* at (3.15)!

So, after assembling the various pieces and executing *MAPLE*'s tensorial linear combination command (`lin.com(coeff1, term1, ...)`) and performing some collections and aesthetic improvements beyond the capacity or inclination of *MAPLE*'s "1000 mathematicians," we obtain:

$$\begin{aligned} \dot{\Omega} = & \beta^\rho \left(\Omega' + \frac{\Omega}{\rho} \right) + \left(\beta^{\rho'} - \frac{\alpha}{\psi^2} \tilde{K}_\rho^\rho \right) \Omega \\ & + \frac{1}{\psi^2 \rho} \left[\alpha'' - \frac{\alpha'}{\rho} + \alpha \left(\sigma'' + \sigma'^2 - \frac{\sigma'}{\rho} + \frac{4\psi''}{\psi} - \frac{4\psi'}{\psi} \left(\frac{\alpha'}{\alpha} + \frac{1}{\rho} + \frac{3\psi'}{\psi} \right) + 8\pi\Phi^2 \right) \right] \end{aligned} \quad (4.20)$$

Given (4.18), the second term may be alternatively expressed as $\Omega \tilde{K}_\theta^\theta$, but as we are not interested in \tilde{K}_θ^θ as a variable, we will leave (4.20) be.

4.3.2 Evolution of the matter fields

As mentioned earlier, the matter itself follows the covariant wave equation,

$$\nabla_\mu \nabla^\mu \phi = g^{\mu\nu} \nabla_\mu \nabla_\nu \phi = 0.$$

As this is a second-order equation, it is convenient for our numerical approach to break it into two coupled first-order equations. In fact, we have already foreshadowed this in (§ 4.2.3) when we defined $\Pi \equiv \psi^2 n^\mu \partial_\mu \phi$; expanding this yields the first of our matter evolution equations:

$$\begin{aligned} \frac{\Pi}{\psi^2} &= n^\mu \partial_\mu \phi = \frac{\dot{\phi}}{\alpha} - \frac{\beta^\rho \phi'}{\alpha} \\ \therefore \quad \dot{\phi} &= \beta^\rho \Phi + \frac{\alpha}{\psi^2} \Pi. \end{aligned} \quad (4.21)$$

As Φ is (for the purposes of the calculation) an "independent" field, we shall also require its evolution; since $\Phi = \phi'$, we can differentiate (4.21) with respect to ρ and

invoke the free commutation of partial time and space derivatives ($[\partial_t, \partial_\rho] = 0$):

$$\begin{aligned}\dot{\Phi} &= \beta^\rho \Phi' + \beta^{\rho'} \Phi + \psi^{-2} \left[\left(\alpha' - \frac{2\psi'}{\psi} \right) \Pi + \alpha \Pi' \right] \\ &= \beta^\rho \Phi' + \left(\frac{\beta^\rho}{\rho} - \alpha \rho \Omega \right) \Phi + \psi^{-2} \left[\left(\alpha' - \frac{2\psi'}{\psi} \right) \Pi + \alpha \Pi' \right]\end{aligned}\quad (4.22)$$

where, for what it's worth, we have used the β constraint (4.18) to eliminate $\beta^{\rho'}$.

For the other decoupled equation, we naturally must return to the wave equation. By the miracles of tensor calculus it may be expressed in a form more conducive to the manipulations we desire to make, *viz.*,

$$\nabla_\mu \nabla^\mu \phi = \frac{1}{\sqrt{-g}} \partial_\nu \left(\sqrt{-g} g^{\mu\nu} \partial_\mu \phi \right) = 0.$$

Carrying out the expansion of this delightful equation with the help of (Eqs. 4.3, 4.21, & 2.4) we obtain

$$\begin{aligned}\dot{\Pi} &= \beta^\rho \Pi' + \Pi \left[\beta^{\rho'} + \beta^\rho \left(\frac{6\psi'}{\psi} + \sigma' + \frac{2}{\rho} \right) - \left(\frac{6\dot{\psi}}{\psi} + \dot{\sigma} \right) \right] \\ &\quad + \frac{\alpha}{\psi^2} \Phi' + \frac{\alpha}{\psi^2} \Phi \left[\frac{\alpha'}{\alpha} + \frac{4\psi'}{\psi} + \sigma' + \frac{2}{\rho} \right]\end{aligned}$$

Into this we substitute the equations for $\dot{\psi}$, $\beta^{\rho'}$, and $\dot{\sigma}$ found earlier. When the dust settles we are left with the comparatively elegant

$$\dot{\Pi} = \beta^\rho \Pi' + \Pi \left(\frac{\beta^\rho}{\rho} - \alpha \rho \Omega - \frac{\alpha}{\psi^2} \tilde{K}_\rho^\rho \right) + \frac{\alpha}{\psi^2} \left[\Phi' + \Phi \left(\frac{\alpha'}{\alpha} + \frac{4\psi'}{\psi} + \sigma' + \frac{2}{\rho} \right) \right]. \quad (4.23)$$

Chapter 5

Supplementary Equations

5.1 Apparent Horizon

The questions that naturally arises in making numerical models of gravitational collapse are, How do we know when a black hole-like object has been created? And how do we convince the computer to ignore it and keep going?

The answer to each of these is the apparent horizon. Whereas the event horizon most physicists (and physics-savvy laymen) are acquainted with is a globally-defined surface, the apparent horizon is subject to a local description. Specifically, the apparent horizon is defined in terms of the local behavior of null, or light-like, rays.

One may imagine, akin to the spirit of Einstein’s famous *gedanken* experiments, a series of concentric shells surrounding the origin of the collapse—the location of the presumptive black hole. At each point on each of these spheres, let there be a point-source of light. If we suppress the angular directions, the light has only two choices: inbound or outbound. The outbound light will form a growing sphere whose progress will be affected by the local gravitational field.

One may imagine, then, if gravity is sufficiently strong, that some of these spherical surfaces of light (“null surfaces”) may not get very far before being stopped and dragged back in to the black hole—paradoxically, even the outbound rays of light are converging. The traditional way of dealing with apparent horizons is to define the

expansion θ as the directional derivative of null geodesics with respect to themselves:

$$\begin{aligned}\theta &\equiv \nabla_v v^\mu = v^\alpha \nabla_\alpha v^\mu; \\ v^\mu v_\mu &= 0.\end{aligned}\tag{5.1}$$

Surfaces for which this quantity is less than or equal to zero are called “trapped surfaces”; the outermost surface where the expansion is zero constitutes the apparent horizon.

In particularly easy cases (such as Schwarzschild), the apparent horizon corresponds exactly to the event horizon, $\rho_{AH} = \rho_{EH} = 2m$. In general, however, the two horizons are distinct, with the apparent horizon always being located within the event horizon¹

Apparent horizons help answer the questions posed at the beginning of this section. They are easily defined in terms of variables a computer is dealing with, without having to look at the whole metric. The formation and existence of an apparent horizon indicates the existence also of a black hole with a central singularity (see, *e.g.*, [31]). The location of the apparent horizon can be used as an excision point, telling the computer to ignore points with $\rho \leq \rho_{AH}$, thus allowing for the evolution outside the black hole to continue beyond the time a black hole is formed.

In the course of testing (5.1) to find the apparent horizon of the Schwarzschild solution (as practice for doing it for our real problem), we found it was actually a rather unwieldy way of going about it. Being that Schwarzschild is just the canonically easy case, this did not bode well.

Fortunately, there is a “back door,” if you will, to apparent horizons in the case of spherical symmetry. Consider again the family of concentric spheres centered at the singularity of a black hole (or where it would form). Each surface is uniquely characterized by its area, and vectors normal to it are manifestly spacelike.

¹ Unless the cosmic censor is taking the day off.

Until, that is, you reach the spheres at which time and space switch their respective timelike and spacelike natures and even outgoing light must converge. When the erstwhile spacelike normal vectors become null, one has reached the outermost trapped surface, which is the apparent horizon.

For Schwarzschild spacetimes the area is the standard $4\pi r^2$, so the norm of the normals to these spherical surfaces is

$$\begin{aligned} g^{\mu\nu} \nabla_\mu(4\pi r^2) \nabla_\nu(4\pi r^2) &= g^{rr} (8\pi r)^2 \\ &= 64\pi^2 r^2 \left(1 - \frac{2m}{r}\right), \end{aligned}$$

which clearly changes signature at $r = 2m$.

Extending this to our situation is relatively easy. Instead of an area, because of the extra dimension our trapped “surfaces” are parametrized by a volume:

$$\mathcal{V} = \oint_{\partial\mathcal{V}} \sqrt{\hat{g}} d^3x \Big|_{\substack{\rho=\rho_0 \\ t=t_0}}$$

It may be remembered that in Table 1 we defined \hat{g}_{AB} as the metric of the reduced manifold on (ζ, θ, φ) , such that

$$dl^2 = \hat{g}_{AB} dx^A dx^B = \psi^4 \left(e^{2\sigma} d\zeta^2 + \rho^2 (d\theta^2 + \sin^2 \theta d\varphi^2) \right)$$

is the line element on the trapped “surface” \mathcal{V} . From this it is evident that the volume element $\sqrt{\hat{g}} = \psi^6 e^\sigma \rho^2 \sin \theta$. Therefore,

$$\begin{aligned} \mathcal{V} &= \int_0^{2\pi} \int_0^\pi \int_0^{2\pi\ell} \psi^6 e^\sigma \rho^2 \sin \theta d\zeta d\theta d\varphi \\ &= 8\pi^2 \ell \psi^6 e^\sigma \rho^2, \end{aligned}$$

because nothing in the integrand (save the $\sin \theta$) depends on the differential coordinates; here we are using ℓ as an unspecified parameter denoting the “size” of the extra dimension ζ .

We wish to find that surface at which the spacelike normals become null, *i.e.*, for which

$$g^{\mu\nu} \partial_\mu \mathcal{V} \partial_\nu \mathcal{V} = 0. \quad (5.2)$$

Since our volume depends only upon t and ρ (making the fairly unphysical assumption that the extra dimension is static in size, *i.e.*, does not and is not expanding with the rest of the universe), this is simple to expand:

$$g^{tt} \dot{\mathcal{V}}^2 + 2g^{t\rho} \dot{\mathcal{V}} \mathcal{V}' + g^{\rho\rho} \mathcal{V}'^2 = 0$$

A little bit of algebra later, we have

$$\left[\left(\frac{\alpha}{\psi^2} + \beta^\rho \right) \mathcal{V}' - \dot{\mathcal{V}} \right] \left[\left(\frac{\alpha}{\psi^2} - \beta^\rho \right) \mathcal{V}' + \dot{\mathcal{V}} \right] = 0$$

The second factor is that which governs the signature of the whole; hence we need only monitor the quantity

$$\chi = \left[\left(\frac{\alpha}{\psi^2} - \beta^\rho \right) \mathcal{V}' + \dot{\mathcal{V}} \right] \quad (5.3)$$

and watch for the tell-tale sign-swap.

We may do something clever with χ : insert the value obtained for \mathcal{V} and expand the derivatives, then replace the time derivatives with their more practical (for purposes of numerical modelling) combinations of spatial derivatives, as dictated by the evolution equations obtained in the previous chapter. Ultimately this yields

$$\chi = 3\beta^{\rho'} \psi^2 + \alpha \tilde{K}_\rho^\rho + (\psi^2 + 2)\alpha\rho\Omega + \frac{2\alpha - 3\psi^2\beta^\rho}{\rho} + \frac{6\alpha\psi'}{\psi} + \alpha\sigma' > 0 \quad (5.4)$$

until the point at which the apparent horizon forms.

5.2 Black Hole Mass

It may also be helpful to know the total mass of any black holes that form. Fortunately, there is an equation, clearly true of the Schwarzschild solution, that may be adapted our model:

$$m = \frac{\rho}{2} \left[1 - \nabla_\mu \left(\frac{A}{A_0} \right)^{\frac{1}{2}} \nabla^\mu \left(\frac{A}{A_0} \right)^{\frac{1}{2}} \right] \quad (5.5)$$

where $A_0 = 4\pi$ is the dimensionless area of a unit sphere. This formula lends itself to a generalization to our case fairly easily, if we replace the A 's with \mathcal{V} 's. In which case,

$$m = \frac{\rho}{2} \left[1 - \partial_\mu \tilde{\mathcal{V}}^{\frac{1}{2}} \partial^\mu \tilde{\mathcal{V}}^{\frac{1}{2}} \right],$$

where $\tilde{\mathcal{V}} = \mathcal{V}/\mathcal{V}_0 = \psi^6 e^\sigma \rho^2$. We have replaced covariant derivatives with their corresponding partials in recognition that a covariant derivative of a scalar reduces to mere partial differentiation. Applying the chain rule, we have

$$m = \frac{\rho}{2} \left[1 - \frac{1}{4\tilde{\mathcal{V}}} g^{\mu\nu} \partial_\mu \tilde{\mathcal{V}} \partial_\nu \tilde{\mathcal{V}} \right]. \quad (5.6)$$

The resemblance to our apparent horizon condition (5.2) is immediately obvious, permitting us to write

$$\begin{aligned} m &= \frac{\rho}{2} \left[1 - \frac{1}{4\tilde{\mathcal{V}}} \left[\left(\frac{\alpha}{\psi^2} + \beta^\rho \right) \mathcal{V}' - \dot{\mathcal{V}} \right] \left[\left(\frac{\alpha}{\psi^2} - \beta^\rho \right) \mathcal{V}' + \dot{\mathcal{V}} \right] \right] \\ &= \frac{\rho}{2} \left[1 - \frac{\chi\xi}{4\tilde{\mathcal{V}}} \right], \end{aligned} \quad (5.7)$$

in which χ is our apparent horizon indicator and ξ is the factor we discarded previously (basically χ with the addition and subtraction interposed).

Chapter 6

The Main Equation Library

At this juncture it may be useful to present and catalog our collection of the constraint and evolution equations we shall use in modelling the dynamical collapse of a scalar field in 4 + 1 dimensions.

So, for your reading pleasure and without further ado, here are the equations more or less as we will be using them in our code:

6.1 Evolution

- Matter

$$\dot{\phi} = \beta^\rho \Phi + \frac{\alpha}{\psi^2} \Pi$$

$$\dot{\Phi} = \beta^\rho \Phi' + \left(\frac{\beta^\rho}{\rho} - \alpha \rho \Omega \right) \Phi + \psi^{-2} \left[\left(\alpha' - \frac{2\psi'}{\psi} \right) \Pi + \alpha \Pi' \right]$$

$$\dot{\Pi} = \beta^\rho \Pi' + \Pi \left(\frac{\beta^\rho}{\rho} - \alpha \rho \Omega - \frac{\alpha}{\psi^2} \tilde{K}_\rho^\rho \right) + \frac{\alpha}{\psi^2} \left[\Phi' + \Phi \left(\frac{\alpha'}{\alpha} + \frac{4\psi'}{\psi} + \sigma' + \frac{2}{\rho} \right) \right]$$

- Metric

$$\dot{\psi} = \beta^\rho \psi' + \frac{1}{2} \left(\beta^{\rho'} - \frac{\alpha \tilde{K}_\rho^\rho}{\psi^2} \right) \psi$$

$$\dot{\sigma} = \beta \sigma' - \beta^{\rho'} + \frac{\alpha}{\psi^2} \left(4\tilde{K}_\rho^\rho + 2\rho \Omega \right).$$

$$\begin{aligned}\dot{\Omega} &= \beta^\rho \left(\Omega' + \frac{\Omega}{\rho} \right) + \left(\beta^{\rho'} - \frac{\alpha}{\psi^2} \tilde{K}_\rho^\rho \right) \Omega \\ &+ \frac{1}{\psi^2 \rho} \left[\alpha'' - \frac{\alpha'}{\rho} + \alpha \left(\sigma'' + \sigma'^2 - \frac{\sigma'}{\rho} + \frac{4\psi''}{\psi} - \frac{4\psi'}{\psi} \left(\frac{\alpha'}{\alpha} + \frac{1}{\rho} + \frac{3\psi'}{\psi} \right) + 8\pi\Phi^2 \right) \right]\end{aligned}$$

6.2 Constraints

$$\beta^{\rho'} = \frac{\beta^\rho}{\rho} - \frac{\alpha \rho \Omega}{\psi^2}$$

$$\tilde{K}_\rho^{\rho'} + \tilde{K}_\rho^\rho \left(\frac{6\psi'}{\psi} + 4\sigma' \right) + 2\Omega (\rho\sigma' - 1) + 8\pi\Phi\Pi = 0$$

$$\alpha'' + \left(\sigma' + \frac{2}{\rho} + \frac{4\psi'}{\psi} \right) \alpha' - 2 \left(3\rho^2 \Omega^2 + 8\rho\Omega \tilde{K}_\rho^\rho + 6\tilde{K}_\rho^{\rho 2} + 4\pi\Pi^2 \right) \alpha = 0$$

$$\frac{\psi''}{\psi} + \frac{\psi'}{\psi} \left[\frac{2}{\rho} + \sigma' + \frac{\psi'}{\psi} \right] + \tilde{K}_\rho^{\rho 2} + \frac{4}{3}\rho\Omega\tilde{K}_\rho^\rho + \frac{1}{2}\rho^2\Omega^2 + \frac{1}{6} \left(\sigma'' + \frac{2\sigma'}{\rho} + \sigma'^2 \right) + \frac{2}{3}\pi(\Phi^2 + \Pi^2) = 0$$

6.3 Supplementary

$$K_A^B = \frac{\tilde{K}_A^B}{\psi^2} \quad \Omega = \frac{\tilde{K}_\theta^\theta - \tilde{K}_\rho^\rho}{\rho}$$

$${}^{(4)}\tilde{K} = \tilde{K}_\rho^\rho + \tilde{K}_\zeta^\zeta + \tilde{K}_\theta^\theta + \tilde{K}_\varphi^\varphi = 0$$

$$\left[\left(\frac{\alpha}{\psi^2} - \beta^\rho \right) \mathcal{V}' + \dot{\mathcal{V}} \right] = 3\beta^{\rho'}\psi^2 + \alpha\tilde{K}_\rho^\rho + (\psi^2 + 2)\alpha\rho\Omega + \frac{2\alpha - 3\psi^2\beta^\rho}{\rho} + \frac{6\alpha\psi'}{\psi} + \alpha\sigma' > 0$$

$$m = \frac{\rho}{2} \left\{ 1 - \frac{2\pi^2\ell}{\mathcal{V}} \left[\left(\frac{\alpha}{\psi^2} + \beta^\rho \right) \mathcal{V}' - \dot{\mathcal{V}} \right] \left[\left(\frac{\alpha}{\psi^2} - \beta^\rho \right) \mathcal{V}' + \dot{\mathcal{V}} \right] \right\} \Big|_{\mathcal{V}=8\pi^2\ell\psi^2\rho^2e^\sigma}$$

Chapter 7

Numerical Approach

7.1 Discretizing Derivatives Into Differences

Difficult manipulations confirm what is painfully apparent at the first cursory glance: the set of equations we have developed are superlatively resistant to analytical solution. Even after the many simplifying assumptions, Killing vectors, and new fields we have introduced, our last and only hope is to turn to computational number-crunching. With all its liabilities and idiosyncracies, numerical differencing is our recourse for integrating the differential equations which represent gravitational dynamics in the presence of an extra spatial dimension.

The main equation library (see previous chapter) is partitioned into evolution and constraint equations in anticipation of the different schemes required to treat the entire set. We shall now briefly describe these.

7.1.1 Evolution

Our overall approach is to use an iterative Crank-Nicholson (*ICN*) differencing scheme for the time-evolution equations. Because we are considering dependence in only one spatial direction, the constraint equations are to be considered as ODEs on every time-slice. To be explicit, we can demonstrate the iterative *ICN* technique on the following model equation:

$$f_{,t} = F(t, \rho, f, f_{,\rho}). \tag{7.1}$$

Because our continuum will be approximated as a discrete set of points, we will adopt a new meaning for super- and subscripts, independent of our former covariant usage, in the context of numerical work. The heretofore continuous position parameter ρ will be replaced by the array ρ_i where the subscript i runs from $0 \dots N$. If the grid spacing is given by h , then ρ_{\max} , representing the outer edge of the grid, will be equal to $N \cdot h$. We do a similar discretization for time (labelling the slices); to distinguish between points on a slice and sequential slices we use a superscript: $t \rightarrow \{t^n\} = n \cdot dt$. A function $f(t, \rho)$ of the continuum variables (t, ρ) in our discretization now becomes

$$f(t^n, \rho_i) \equiv f_i^n. \quad (7.2)$$

The toy-model equation (7.1), expressed via *ICN* differencing, is now

$$\frac{f_i^{n+1} - f_i^n}{dt} = \frac{1}{2} (F_{i+1}^{n+1} + F_{i-1}^{n+1}) + \frac{1}{2} (F_{i+1}^n + F_{i-1}^n) \quad (7.1')$$

Note that on the right hand side we have averaged the source term at both the n and the $n + 1$ time levels. This differencing scheme is second-order in space and time with respect to the point-event at $(t^{n+\frac{1}{2}}, \rho_i)$. Equation (7.1') can be “solved” for f_i^{n+1} :

$$f_i^{n+1} = f_i^n + \frac{1}{2} \left\{ (F_{i+1}^{n+1} + F_{i-1}^{n+1}) + (F_{i+1}^n + F_{i-1}^n) \right\} dt.$$

However, this is an implicit scheme, as we have the appearance of the advanced time level (f^{n+1}) on both the right and left-hand sides, and on the RHS it is buried inside the F . To solve this we would need something akin to a matrix solver. As even in one dimension this is computationally expensive, we modify this implicit scheme to make it explicit. In particular, we use the value of f^n, f_ρ^n at the n time level to get an initial approximation for the $n + 1$ time level, ${}^{(0)}F_i^{n+1} = F_i^n$. We then substitute this “static-evolution” guess into the mess on the RHS and find a better approximation for

f_i^{n+1} , call it $^{(1)}f_i^{n+1}$. This “first iteration” of f we substitute into the RHS to obtain $^{(1)}F_i^{n+1}$ and thus a better value for f_i^{n+1} , call it $^{(2)}f_i^{n+1}$. We thus iterate repeatedly using the latest value for f_i^{n+1} , until the k^{th} iteration, $^{(k)}f_i^{n+1}$, is within some specified tolerance of the previous iteration, $^{(k-1)}f_i^{n+1}$.

This is the basic strategy for each of the evolutionary equations. It is worth pointing out that the source terms, which we have consolidated under the beguilingly simple label F , are functions of other variables besides the one being integrated.

7.1.2 Constraints

For the non-hyperbolic (elliptic) “constraint” equations, comprising the equations for α (from the slicing condition), ψ (from the Hamiltonian constraint), \tilde{K}_ρ^ρ (from the momentum constraint), and β (from the definition of \tilde{K}_ρ^ρ), different strategies are required.

Both the α and ψ equations are second-order of the general form

$$f_{,\rho\rho} + Af_{,\rho} + Bf = S,$$

where A , B , and S are nonlinear combinations of the “other” variables. Thus, despite the overt hideousness of these equations (see chapter 6), their structure is actually much like that of the ordinary second order differential equations one learns about in introductory calculus.

Pleasant as the overall form is, as stated earlier, solving these equations analytically is not a realistic option, so we turn to computational methods augmenting the ones employed for the evolution equations. Our strategy for these second-order equations is to use centered-differencing in the space of the function f (be it α or ψ) while allowing the coefficients A, B, S to be evaluated at the point ρ_i in the following

manner:

$$\frac{f_{i+1}^n - 2f_i^n + f_{i-1}^n}{h^2} + A_i^n \frac{f_{i+1}^n - f_{i-1}^n}{2h} + B_i^n f_i^n = S_i^n.$$

Note again that everything occurs at a single time level. This can be recast in a form that is suggestive of matrix manipulations:

$$\left(\frac{1}{h^2} - \frac{A_i^n}{2h}\right) f_{i-1}^n + \left(-\frac{2}{h^2} + B_i^n\right) f_i^n + \left(\frac{1}{h^2} + \frac{A_i^n}{2h}\right) f_{i+1}^n = S_i^n \quad (7.3)$$

Define the vector (in a different vector space than the world of the Einstein equations where we worked in the preceding) of function-values \vec{f}^n and the source values \vec{S}^n . We can then represent the mess above as the simple matrix equation

$$M \vec{f}^n = \vec{S}^n,$$

where M is a tridiagonal matrix whose nonzero elements correspond to the indexed coefficients in (7.3). Our solution, then, reduces to the solution of the above matrix equation for \vec{f}^n . Fortunately, tridiagonal equations are not as expensive to solve as generic matrix equations owing to their sparseness and the symmetry of their form. Indeed, there are a number of canned routines extant that perform this inversion; one of which we borrowed rather than write our own.

This approach works for α and ψ ; for the first order \tilde{K}_ρ^ρ and β equations we can do a straightforward integration of the form

$$f' = F$$

$$\frac{f_{i+1}^n - f_i^n}{h} = \frac{1}{2} (F_{i+1}^n + F_i^n)$$

where we have again done a slick averaging to obtain an equation second order with respect to the point $(t^n, \rho_{i+\frac{1}{2}})$.

The order in which we perform these operations makes a difference that must be accounted for. In particular, the α and β equations, as a pair, decouple from the \tilde{K}_ρ^ρ and ψ equations; which is to say that the equations for \tilde{K}_ρ^ρ and ψ do not depend upon α or β . Furthermore, α 's equation contains no mention of β . This suggests a natural order in which to perform the integrations: we will first integrate \tilde{K}_ρ^ρ and ψ (iteratively, as they do not decouple from each other). Once \tilde{K}_ρ^ρ and ψ are known, it is natural to treat α next. Finally, we integrate β .

7.2 Boundary Conditions

Up to this point we have assiduously avoided mention of the silent partner in any well-posed differential equation problem. Now, therefore, is a critical time to discuss the boundary conditions we should like to employ.

First (because they're easier), we deal with the BC's for the constraint variables. At $\rho = 0$, regularity conditions (see § 3.1.1) demand that α and ψ be even functions of ρ . As a result, we can take as boundary conditions the vanishing of their first derivatives:

$$\left. \frac{\partial \alpha}{\partial \rho} \right|_{\rho=0} = \left. \frac{\partial \psi}{\partial \rho} \right|_{\rho=0} = 0;$$

or in other words, that α and ψ are subject to homogenous Neumann conditions at the origin. Since the equations for α and ψ are second-order, we need an additional condition for complete determination thereof. Here things become a little more subtle (which is physics-speak for “nasty”). Physically, we assume that the far-field regime approximates Minkowski space.¹ This is known as “asymptotic flatness.” For the

¹ Of course, in five dimensions this amounts to only a guess.

lapse and conformal factor this implies that both should take the form

$$1 + \frac{C(t)}{\rho} + \mathcal{O}(\rho^{-2}) \tag{7.4}$$

far from the origin. Thus, if we were integrating all the way out to spatial infinity, our boundary conditions would be that both α and ψ go to unity. In practice this is not the case, as we are truncating our spatial grid at a “large” but nonetheless very finite value. As a result, we have no right to expect either α or ψ to be equal to unity at the outer edge of the grid. Thus it would be nice to find a correction to the boundary condition that reflects its expected far-field behavior. The above form (7.4) provides such a possibility. Using ψ as an example, we can rewrite the asymptotic condition as

$$[\rho(\psi - 1)]_{,\rho} \sim \mathcal{O}(\rho^{-2}). \tag{7.4'}$$

Provided that our outer edge, ρ_{\max} , is “sufficiently” far away to be in the asymptotic regime, our condition becomes the Robin (‘ro-BAN’) condition, otherwise expressed as

$$\psi + \rho \psi_{,\rho} |_{\rho_{\max} \gg 1} = 1.$$

Unfortunately, application of this BC to ψ proves to be unstable for reasons that are still unclear. As a result, we are forced to default to the simple Dirichlet condition rejected previously, which gives us decent results but also pause. Partly as a result, we tended to use a rather large grid with the hope that the outer boundary was well within the asymptotic regime and that therefore the Dirichlet approximation was sufficiently faithful to reality.

For our quantities β^ρ and \tilde{K}_ρ^ρ , which satisfy first-order ODEs, but one boundary condition is needed. In both cases, we chose to use the asymptotic condition, in which both β^ρ and \tilde{K}_ρ^ρ vanish at spacelike infinity, and integrate inward. Again,

because of the finite size of our grid, the use of this homogeneous Dirichlet BC is an approximation which strictly needs a correction. In this case, that correction is provided for both by the value of the function at $\rho = 0$; for both functions, regularity demands that they vanish at $\rho = 0$. This however is not to be treated or considered as an over-determining BC: the actual, near-scandalous, operation is to integrate from the outside in, find the variation from zero at the origin, and then offset the entire function by exactly that much in the opposite direction.

For the evolution equations, we will use regularity at $\rho = 0$ (technically, then, this is an initial-boundary value problem). Regularity demands that certain functions be even or odd and have corresponding homogeneous Neumann or Dirichlet boundary conditions:

$$\begin{array}{rcl} \sigma'(0) & = & 0 \\ \phi'(0) & = & 0 \\ \Pi'(0) & = & 0 \end{array} \quad \begin{array}{rcl} \Omega(0) & = & 0 \\ \Phi(0) & = & 0 \end{array}$$

Second-order equations require two conditions; the natural place to put the other member of the pair is at the outer edge, and as these are wave-like equations, the natural choice is some sort of “outgoing wave” condition.

The simpler variables are those relating to the scalar field. Using flat space as our example, we expect that the solution to the general flat space wave equation in spherical coordinates is just

$$\frac{1}{\rho} (f(t - \rho) + g(t + \rho)),$$

where we think of f as the outbound, and g as the inbound wave. The imposition of outgoing wave boundary conditions is found in simply requiring that $g = 0$, or that $\phi = \frac{f(t-\rho)}{\rho}$ (ϕ being our canonical example here). If this is the case, simple

manipulations reveal that the correct outgoing wave condition can be written as

$$(\rho\phi)_{,t} = -(\rho\phi)_{,\rho}.$$

In this case, we will impose exactly this condition for the scalar fields, although one would imagine, again, that this is true only in the asymptotic regime where spacetime is essentially flat.

For the remaining two variables, life (which continues beyond the boundary) is more complicated. We have equations for σ and Ω , which are first order in time but second order in space. The latter can be seen in the $\dot{\Omega}$ equation, in which there are second derivatives of σ .

We'll need a characteristic decomposition, and find the ingoing and outgoing wave components of a generic solution. To get this characteristic decomposition we need a strictly first-order system in both time and space. Hence we must introduce the variable $\eta \equiv \frac{\sigma'}{\rho}$. To get the relevant behavior of our gravitational waves, we will assume that these variables are nontrivial but that all other undifferentiated metric components are constant.

Then the evolution equations, decoupled, and with all appropriate substitutions made (for there are terms that show up that can be simplified in terms of our other “dynamic” variables), become

$$\begin{aligned} \dot{\sigma} &= 0 & + \dots \\ \dot{\Omega} &= \beta^\rho \Omega' + \frac{1}{3} \frac{\alpha}{\psi^2} \eta' & + \dots \\ \dot{\eta} &= \beta^\rho \eta' + 3 \frac{\alpha}{\psi^2} \Omega' & + \dots \end{aligned}$$

This, of course, may be cast into a matrix formulation in the vector $H = [\sigma, \Omega, \eta]^T$ as follows:

$$\dot{H} = AH' + B$$

$$\begin{bmatrix} \sigma \\ \Omega \\ \eta \end{bmatrix} \bullet = \begin{bmatrix} 0 & 0 & 0 \\ 0 & \beta^\rho & \frac{1}{3} \frac{\alpha}{\psi^2} \\ 0 & 3 \frac{\alpha}{\psi^2} & \beta^\rho \end{bmatrix} \begin{bmatrix} \sigma \\ \Omega \\ \eta \end{bmatrix}' + \begin{bmatrix} \dots \\ \dots \\ \dots \end{bmatrix} \quad (7.5)$$

where, of course, A represents the coefficients on the derivatives, and B is a column vector containing all the “extra” terms that do not involve the components of H .

The primary behavior of H is governed by the derivatives, so we will, for the purposes of finding the boundary conditions here ignore B from now on. Furthermore, let it be remembered that although the fields α, β^ρ , and ψ that appear in the matrix A are in general variable, for points “close enough to infinity” we are assuming these functions take on an asymptotic constancy with respect to ∂_ρ and ∂_t .

Wavelike solutions to this linearized set of equations, $H \simeq H_0 e^{i(k\rho \pm \omega t)}$, are assumed to exist; some little manipulations of our matrix equation using this ansatz yields

$$\left(A \mp \frac{\omega}{k} \mathbf{1} \right) H = 0,$$

the classic eigenvalue problem, with the eigenvalues $\frac{\omega}{k}$ being the characteristic velocities, and the eigenvectors $H_{(0,+,-)}$ being the characteristic waveforms, which will give us (assumedly) the far-field behavior, and thus our outer boundary condition.

Carrying out the eigencalculation in the eigenway, we obtain (as alluded to briefly in the preceding paragraph) the eigenvelocities $\{0, \beta^\rho \pm \frac{\alpha}{\psi^2}\}$ with corresponding non-normalized eigenvectors

$$H_{(0)} = \begin{bmatrix} 1 \\ 0 \\ 0 \end{bmatrix}; \quad H_{(+)} = \begin{bmatrix} 0 \\ 1 \\ 3 \end{bmatrix}; \quad H_{(-)} = \begin{bmatrix} 0 \\ 1 \\ -3 \end{bmatrix}.$$

The aggregate of these vectors, in a 3×3 matrix, is recognizable as the inverse of the diagonalizing matrix,

$$R^{-1} = \begin{bmatrix} 0 & 1 & 0 \\ 1 & 0 & 1 \\ 3 & 0 & -3 \end{bmatrix}.$$

If we multiply our linearized (far-field regime) matrix equation (7.5) by R , we get

$$\begin{aligned} R \dot{H} &= R A H' \\ (\dot{R}H) &= (R A R^{-1}) (RH)' \end{aligned} \quad (7.6)$$

because R consists entirely of constants.

The quantity we really want is $v = RH$, consisting of the characteristic variables:

$$v_1 = \frac{1}{6}(3\Omega + \eta); \quad v_2 = \sigma; \quad \text{and} \quad v_3 = \frac{1}{6}(3\Omega - \eta).$$

Their respective wave equations (7.6) are simple to solve, since by the properties of linear algebra, the matrix R thus applied to A renders it diagonal.

The diagonal elements, identical to the eigenvalues of course, become the characteristic velocities of these eigenwaves, to wit,

$$\dot{v}_1 = \left(\beta^\rho + \frac{\alpha}{\psi^2} \right) v'_1; \quad \dot{v}_2 = 0; \quad \text{and} \quad \dot{v}_3 = \left(\beta^\rho - \frac{\alpha}{\psi^2} \right) v'_3; \quad (7.7)$$

which are classical advection equations with characteristic velocities equal to the eigenvalues found previously. From these we see that $v_2 = \sigma$ is static (for $\rho \gg 0$). The far-field behavior of the other two eigenvelocities tends towards ± 1 , because the shift $\beta^\rho \rightarrow 0$ while both the lapse and conformal factor $\alpha, \psi \rightarrow 1$.

Keeping in mind, of course, that this linearized approach is assumed to be valid only far from the origin, it is nonetheless interesting to note that at some closer point even the outgoing wave's velocity may become negative—a signature of a “black” region. Practically speaking, in the code the greater of the characteristic velocities is used as the Courant limit, or the maximum speed at which information can move between grid points.

It is a simple mental exercise, therefore, to convince oneself that v_3 represents an outgoing wave at infinity ($v_3(t - \rho)$ satisfies $\dot{v}_3 = -v'_3$), and v_1 , the inbound wave. Our

outer boundary condition, then, is simply to kill the *ingoing* characteristic variable $v_1 = \frac{1}{6}(3\Omega + \eta)$.

Expressing our true variables in terms of the characteristic variables v_i ,

$$\Omega = v_1 + v_3; \quad \frac{1}{3}\eta = v_1 - v_3,$$

the application of our $v_1 \rightarrow 0$ boundary condition means that

$$\begin{aligned} \Omega &= v_3 \left(\rho + (\beta^\rho - \alpha/\psi^2)t \right) \\ \frac{\eta}{3} &= -v_3 \left(\rho + (\beta^\rho - \alpha/\psi^2)t \right) \end{aligned}$$

Therefore, Ω must obey v_3 's advection equation at the outer boundary: $\dot{\Omega} = \left(\beta^\rho - \frac{\alpha}{\psi^2} \right) \Omega'$.

Meanwhile, we can get away with telling the computer that $\sigma' = \rho\eta = -3\rho\Omega$ at the furthest point(s) on the grid.

Strictly speaking, this maneuvering serves only to inform the code about the dynamic behavior of the fields at the outer boundary—that no waves ought to be reflected, let alone be spontaneously generated, at ρ_{\max} . There is another issue that is easily addressed: the falloff with distance. Again, in five dimensions this amounts to only a guess, but it is reasonable to suppose (and the convergence tests make no large complaint) that the fields drop off as ρ^{-1} ; i.e., that the “true” field behavior is sufficiently approximated by $\Omega \sim \frac{1}{\rho}\Omega_{\text{guess}}$, where Ω_{guess} represents the Ω obtained in the foregoing boundary condition considerations.

7.3 Convergence Testing

We use center-differenced approximations wherever possible, as this is second-order accurate:

$$\frac{\partial\psi}{\partial x} \approx \frac{\psi_{i+1} - \psi_{i-1}}{2h} + \mathcal{O}(h^2).$$

It is a central assumption to numerical differencing that the numerical solution ψ_h , obtained at a resolution level $dx = h$, differs from the “true” solution by a small, second-order quantity, i.e., $\psi_h = \hat{\psi} + \mathcal{O}(h^2) = \hat{\psi} + \varepsilon h^2$. In like manner, were we to double the grid spacing to $2h$, and again to $4h$, it is assumed that this doubling will propagate through so that

$$\begin{aligned}\psi_{2h} &= \hat{\psi} + \mathcal{O}((2h)^2) = \hat{\psi} + \varepsilon(4h^2) \\ \psi_{4h} &= \hat{\psi} + \mathcal{O}((4h)^2) = \hat{\psi} + \varepsilon(16h^2)\end{aligned}$$

Now, if our differencing code is faithfully representing our differential equations, then the numerical solutions ought to be converging to the “true” solution at higher resolution, which is to say smaller grid spacing. To determine whether this is happening, it is instructive to take the ratio of the differences between the numerical solutions for different resolutions.

$$\frac{|\psi_{4h} - \psi_{2h}|}{|\psi_{2h} - \psi_h|} = \frac{\varepsilon(16h^2 - 4h^2)}{\varepsilon(4h^2 - h^2)} = 4.$$

Included in our program-package is a set of “initial data” files, `id0`, `id1`, `id2`, ..., where each one has double the resolution of the last, *e.g.*, whereas `id3` has $4097 = 1 + 2^{12}$ grid points, `id4` has half the spacing for a total of $8193 = 1 + 2^{13}$ grid points. In general, `idN` has $1 + 2^{9+N}$ data points. (Naturally, the higher the resolution level, the longer the computation run lasts. Level 3, for instance, typically takes less than an hour, while a run at level 5 takes the better part of a day on the computers available to us.)

There is also a pre-existing program that takes runs at three different levels (say, 3, 4, and 5), and computes the ratio of the differences in the solutions. The closer the result is to a string of fours (or a horizontal line at four when plotted), the greater

our assurance that the code is converging to a correct solution. A sample of our convergence test is provided in Figure 7.1.

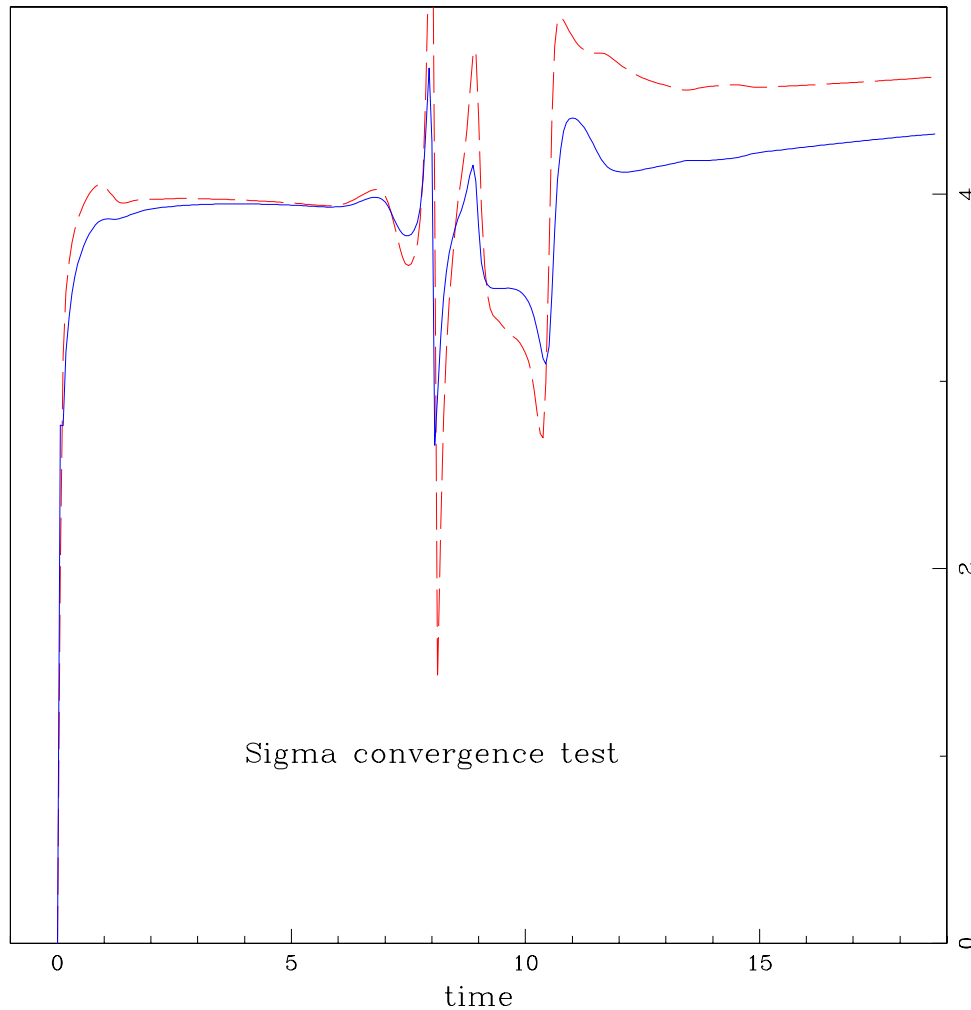


Figure 7.1 — Two convergence test results for σ at $\{\text{id2}, \text{id3}, \text{id4}\}$ (dashed) and $\{\text{id3}, \text{id4}, \text{id5}\}$ (solid) in a dispersive case ($\sigma_0 = 0.1$). The ratio of level-differences tends to be near 4 for most of the time; this gives us reasonable confidence that our code is convergent to the “real” solution.

The time span represented here was not sufficiently long for the outgoing wave to reach the outer boundary. The “noise” at $7 < t < 13$ therefore arises when the inbound wave hits the origin, and is an indication that our boundary conditions at $\rho = 0$ are not perfect. Nevertheless, it is clear that the noise is dampened in successively finer resolution-triads, and is “close enough” to four to suit our purposes.

Chapter 8

Results and Interpretations

We achieved some rather remarkable results. One area of intrigue was the window of criticality, *i.e.*, the region of phase-space (with respect to the field’s initial amplitudes), where the system must “decide” whether it will become a black string, or disperse into nothing interesting.

Of particular interest was whether or not the system exhibited the critical phenomena, especially self-similarity, noted in previous numerical simulations of $3 + 1$ spacetime by Choptuik and others, as described in (§ 1.1.4) of this thesis.

And apparently we are not alone in this our interest; for a paper [32] posted on lanl.gov’s *arXiv* just days before the completion of this thesis presents much the same work (albeit in many fewer pages). The authors seem to have found an even stronger case for discrete self-similarity in $4 + 1$ pure gravitational collapse. It is encouraging to see corroboration from our colleagues, albeit disappointing to be thus “scooped,” or beat to the punch.¹

Our initial data files call for, and therefore allow user-controlled variation in, the initial amplitude of both the scalar field $\phi = \phi_0 e^{-\left(\frac{\rho-\rho_0}{\delta\phi}\right)^2}$ and the logarithm of the ζ -scaling, $\sigma = \sigma_0 e^{-\left(\frac{\rho-\rho_0}{\delta\sigma}\right)^2}$. For the sake of code exploration, we decided to set each

¹Upon closer investigation, it appears the “scooping” is not as complete as was initially feared; the problem addressed in [32] concerns the relaxation of a distorted $SO(3)$ spherical spacetime—a similar idea to that which we use here, but sufficiently different as to leave our approach, for the moment, unique.

initial amplitude to zero in turn, in order to investigate the contributions of each field separately.

8.1 Scalar Field Collapse

The results for the scalar field were not as interesting as those for the gravitational field. It may satisfy the reader's interest, therefore, to merely note that the critical amplitude for collapse of a massless scalar field is $\phi_0 \approx 0.0275$. Table 2 shows the margin of criticality for the collapse of a massless scalar field, with an initial σ of zero. Naturally, during the course of the evolution σ leaves zero because, according to the Einstein equations, the matter affects the metric of spacetime.

Resolution	Critical amplitude	Precision
4097	$\phi_0 = 0.02725 \pm 5E-5$	$\pm 0.183\%$
8193	$\phi_0 = 0.0275655 \pm 5E-7$	$\pm 0.00184\%$
16385	$\phi_0 = 0.02775 \pm 5E-5$	$\pm 0.180\%$

Table 2

The critical point for ϕ remained, as would be hoped for, approximately constant as we went to increasing levels of resolution, drifts upward slightly as we used finer grids; whether this is a purely numerical effect or not remains as yet unknown.

We could have dug deeper into all `id` levels, but felt it was sufficient to stop at $\Delta\phi/\phi < 1\%$ at resolution levels 3 and 5 (4097 and 16385 points respectively), and at $\Delta\phi/\phi < .02\%$ in the case of 8193 points. It is impressive how the development of a black hole final state is so exquisitely sensitive to initial conditions, one part in tens of thousands makes a difference! Certainly, one might expect that there would be a specific point of criticality (such is what we set out looking for, after all), but to

actually find it so precisely brings a sense of awe.

8.2 Gravitational Field Collapse

Our greater interest was in studying the behavior of the system in the absence of matter, *i.e.*, pure gravitational collapse. It should be stressed that this is a uniquely five-dimensional effect, as the only thing allowed to “collapse” from an initial state was a spherical gaussian pulse, $\sigma = \sigma_0 e^{-\left(\frac{\rho-\rho_0}{\delta\sigma}\right)^2}$ —a localized distortion in an otherwise flat spacetime.

Granted, how one might physically arrange to have a spherical pulse of spacetime distortion in the first place is one of those imponderables of purely theoretical physics. Nevertheless, our findings, as well as those in [32], suggest that were such an unlikely configuration to spring into existence somewhere, and were it strong enough, there could form a black hole—composed entirely of nonmaterial gravity—at the center of the shell. A black hole composed of nothing but gravity is enough to tantalize any imaginative physicist.

As in scalar field collapse, gravitational field collapse has a critical point. Since making black holes out of pure gravity is much more intriguing, we delved deeper into the window of criticality and thus discovered some fascinating behavior, some or all of which has yet to be explained from the equations.

Resolution	Critical amplitude	Precision
4097	$\sigma_0 = 0.119375 \pm 5.625\text{E-}3$	$\pm 4.712\%$
8193	$\sigma_0 = 0.114144395 \pm 5\text{E-}9$	$\pm 4.38\text{E-}6\%$
16385	$\sigma_0 = 0.1141337109 \pm 3\text{E-}10$	$\pm 2.63\text{E-}7\%$

Table 3

Again, we emphasize the incredible sensitivity to the initial amplitude—one part in a billion! We have no doubt that, were it desired (if by no more than sheer curiosity), we could push this all the way down to machine precision. Again, this is not so much an astonishment but a startling confirmation of what we had intuited from the beginning. After all, the system has to take exactly one of exactly two options as a final state.

All this aside, the sensitivity is the *least* interesting thing about gravitational field collapse. One much more intriguing observation we made is that the closer the initial field is to criticality, the sooner the black string forms.

In other words, a σ_0 of .25 lags behind, and forms a black string later than, a σ_0 of .15, and so on down to the critical amplitude. This pattern holds true independent of the grid resolution and baffles myself, my advisor, and Dr. Nielsen of the BYU physics department. This dynamic is shown in the following four figures, all from data generated at `id3`, or on a grid of 4097 points.

The first (Fig. 8.1) shows the evolution of $\sigma(t, \rho)$ for three initial amplitudes, $\sigma_0 = .25$ (solid line), $\sigma_0 = .20$ (dotted), and $\sigma_0 = .15$ (dashed). All of these amplitudes are well within the black-string-formation domain (see Table 3).

Most intriguingly, the “weaker but quicker” field is also the only one of the three to transpire in the positive range, something made even clearer in Figure 8.3. One wonders if quick death and an upwardly-mobile σ (that even breaches $\sigma = 0$) are related.

The second (Fig. 8.2) illustrates the evolution of the lapse—in a sense, it is a picture of the evolution of time, since physically α answers to the rate at which a test-point moves from one spatial slice to the next. Thus, when α reaches zero (or gets really close), time has essentially stopped at that locale. While we did not have time to implement the apparent horizon or mass equations, a very small α (and gradients

that caused the program to quit) serve as good enough indications of black string formation. Again, we see that the weaker initial field reaches a black-string state sooner.

Even stranger, it appears that the value of the lapse α at the origin passes through a certain value (≈ 0.67) at a particular time (≈ 7.5) *regardless of the initial amplitude of the collapsing gravitational wave!* This mysterious phenomenon is shown in Figure 8.4.

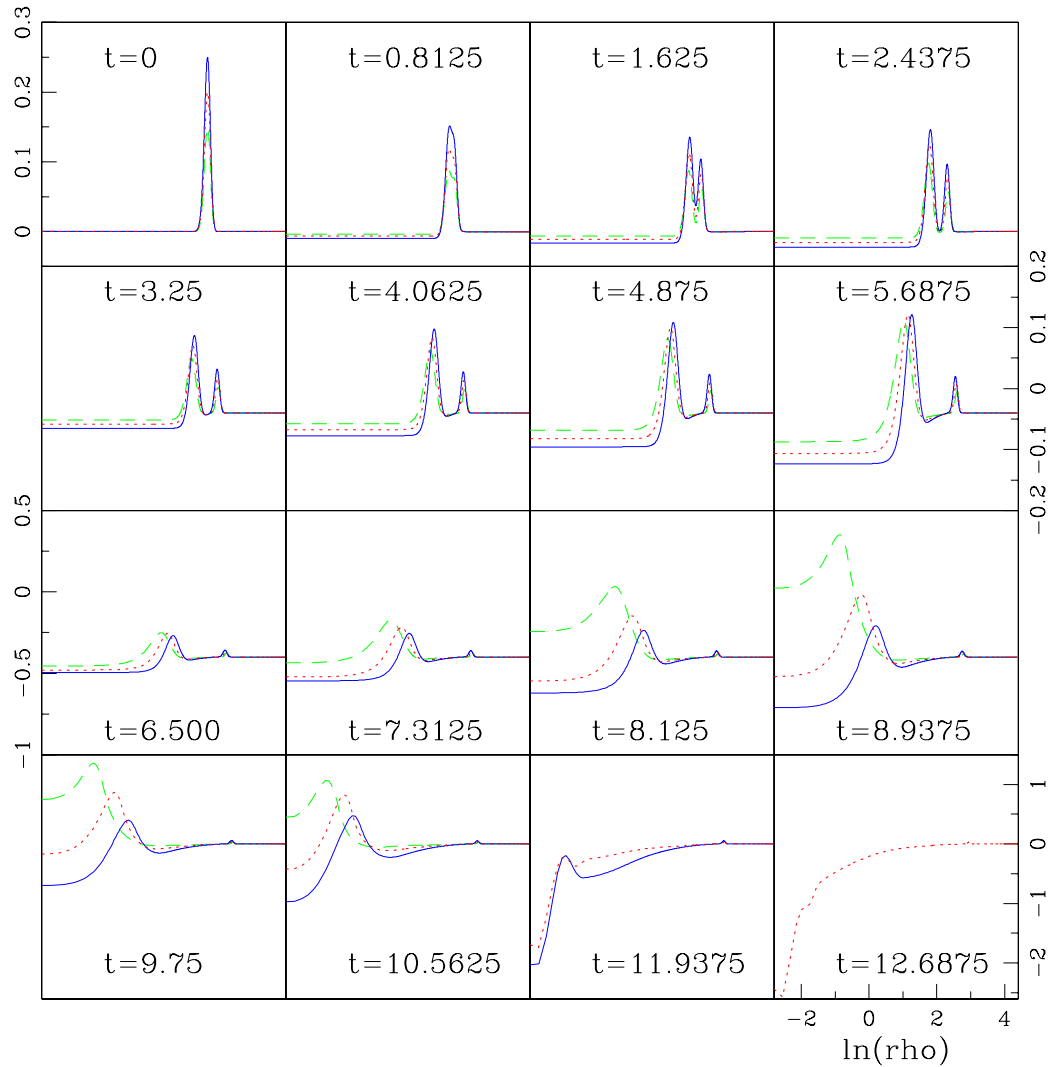


Figure 8.1 — Semilog plot of $\sigma(t, \rho)$ for three initial amplitudes. The vertical scale for each row has been adjusted to allow easy visualization of the field at all times. The weaker initial amplitude (dashed) collapses faster and is the first to make a black string.

(Figs. 8.1-8.4) are shown as semilog plots, or a plot of the function with respect to the logarithm of ρ , in order to magnify the action near the origin for our viewing pleasure.)

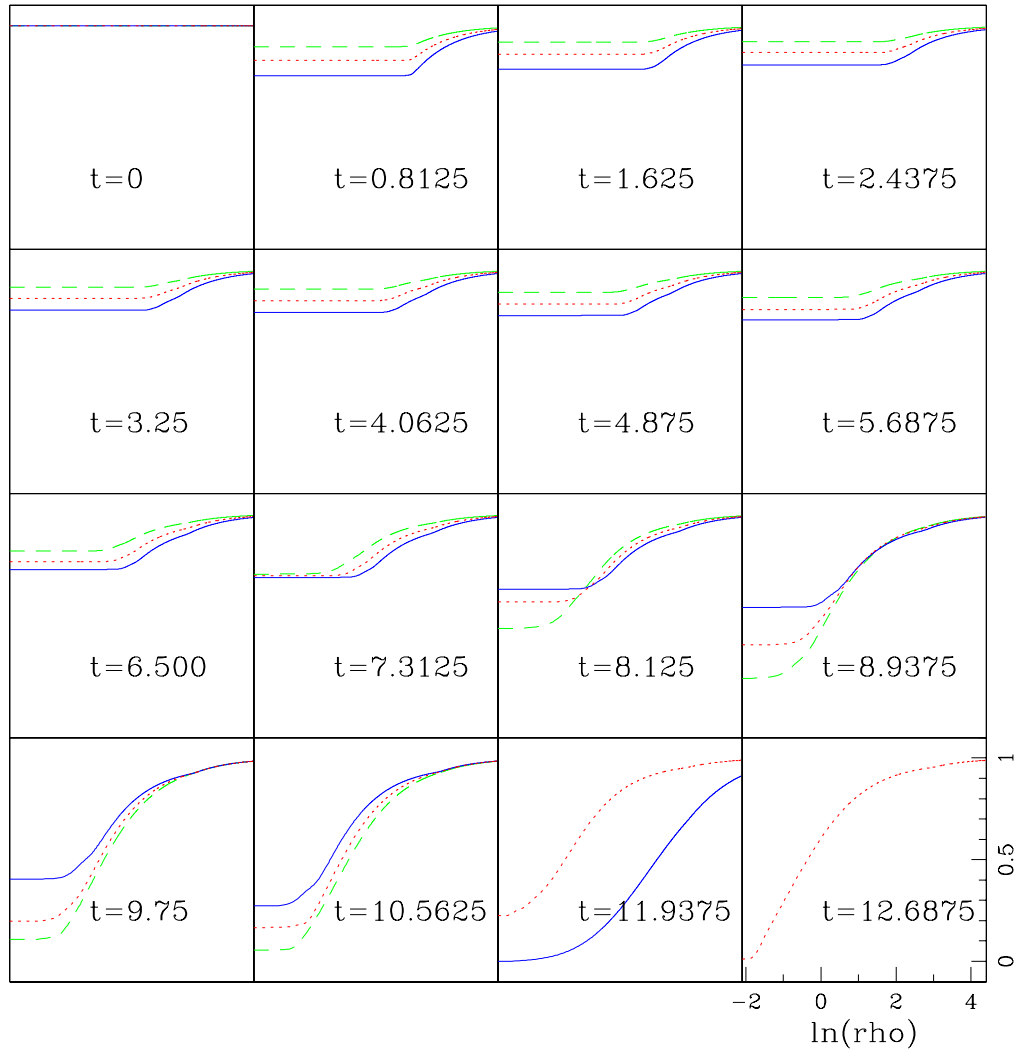


Figure 8.2 — Semilog plot of $\alpha(t, \rho)$ for three initial amplitudes. The weaker initial amplitude (dashed) collapses faster and is the first to approach zero, indicating the formation of a black string.

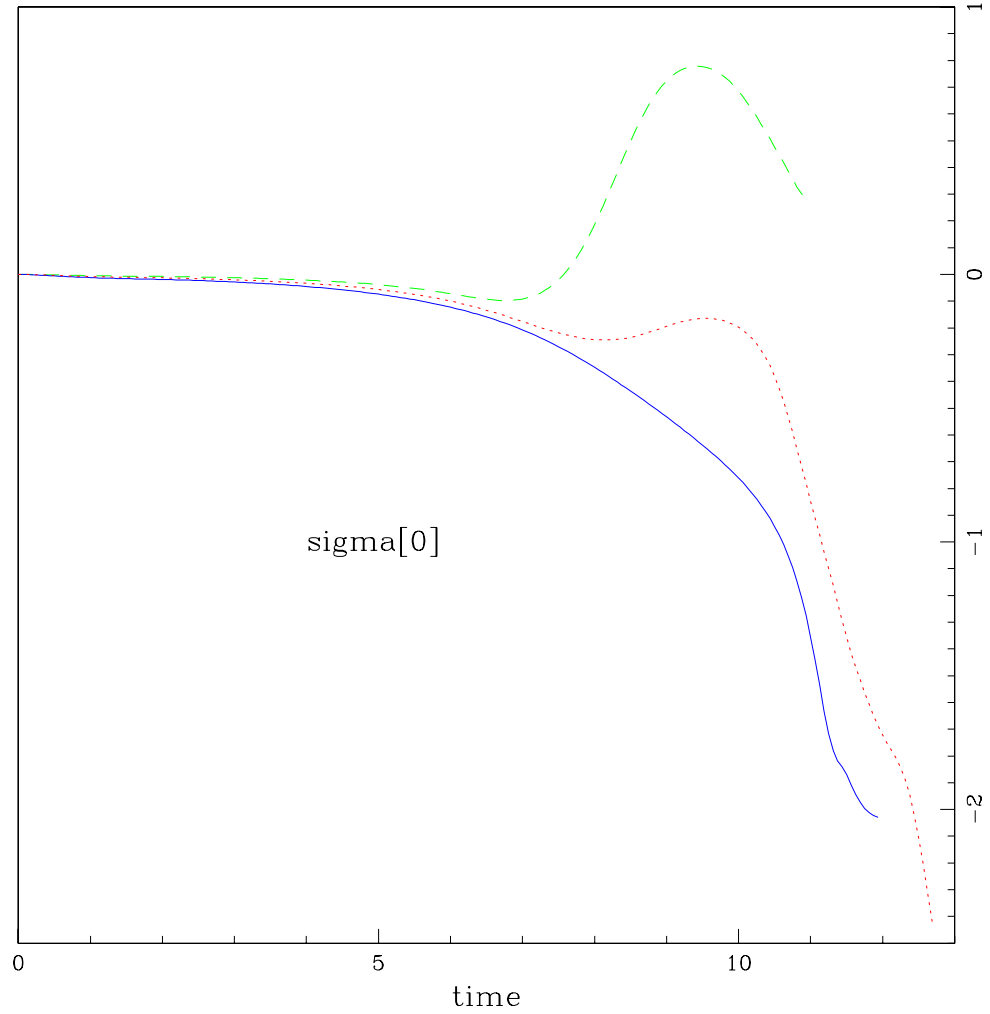


Figure 8.3 — Time plot of $\sigma|_{\rho=0}$ for three initial amplitudes. The weaker initial amplitude (dashed) collapses sooner, and is the only one to die in the positive regime. Is there a relation between a $\sigma(0) > 0$ and rapid black string formation?

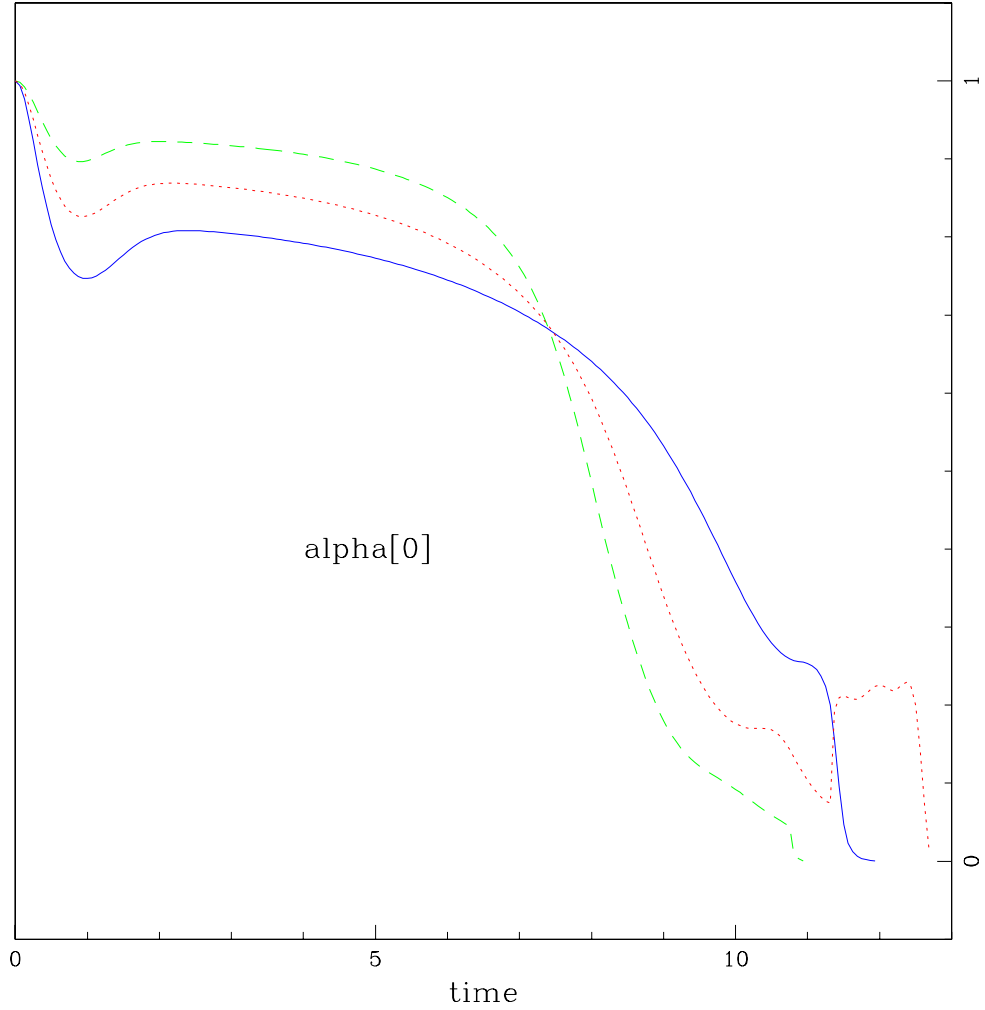


Figure 8.4 — Time plot of $\alpha|_{\rho=0}$ for three initial amplitudes. For some reason yet to be determined, the value of $\alpha(0)$ at a particular time in the evolution is independent of the initial amplitude of original the gravitational field. This phenomenon persists at higher resolution levels.

Finally, we look at two evolutions, for initial field strengths at the respective edges of the extremely narrow critical window for `id5`. Even with the semilog plot, and even with a compression of frames favoring the latter half of the evolution, so close to each other are the initial data that the evolutions are virtually indistinguishable until $t=12.125$.

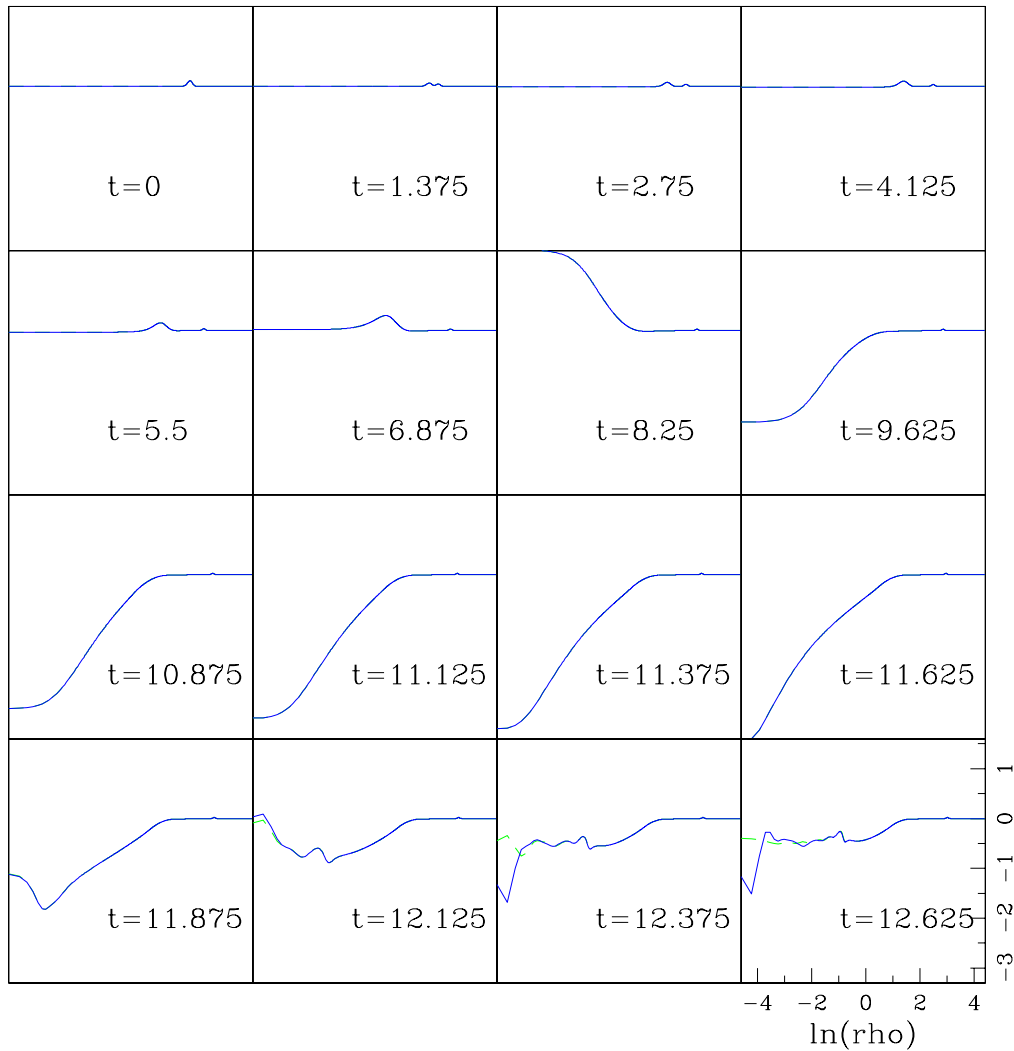


Figure 8.5 — The supercritical (solid line) and subcritical (dashed) evolutions of σ at $100 \pm 2.63E-7\%$ of the critical amplitude. In the final frame, there are indications of self-similarity manifest in the “self-echoing” of the outbound shock wave. An adaptive grid would be needed to tell for certain.

The most interesting feature of this pair is the self-echoing visible in the left half of the final frame (see Fig. 8.5). Also, in (Fig. 8.6) we get this really strange kink in α .

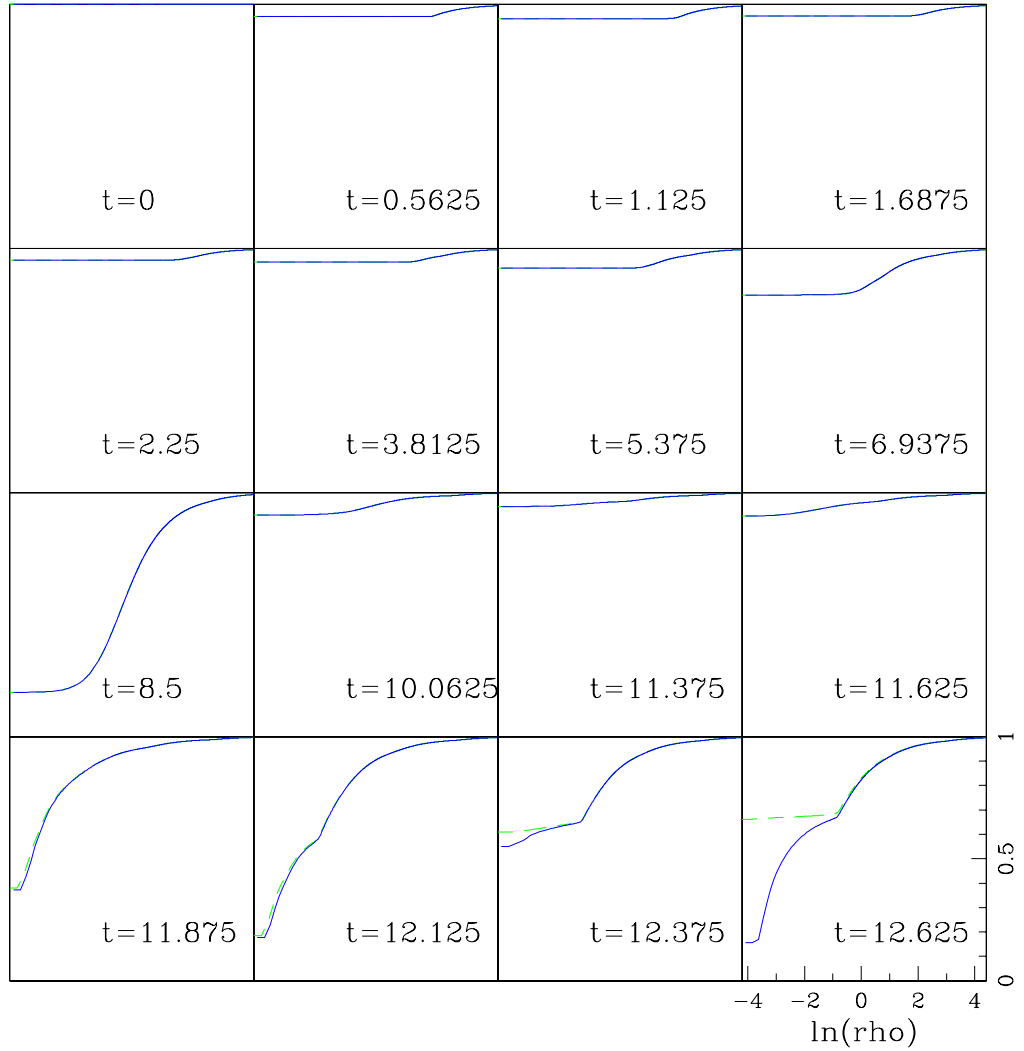


Figure 8.6 — The supercritical (solid line) and subcritical (dashed) evolution of α at $100 \pm 2.63\text{E-}7\%$ of the critical amplitude. What's with the kink?

Finally, we look at the super- and subcritical behavior of α at the origin. Two things to notice here are the bouncing as the “moment of decision” is approached, and the general structure of the curve—something that we didn’t get to see in the plots of collapse far from criticality. The critical road to a black string state is not exactly what one would call monotonic, or even smooth.

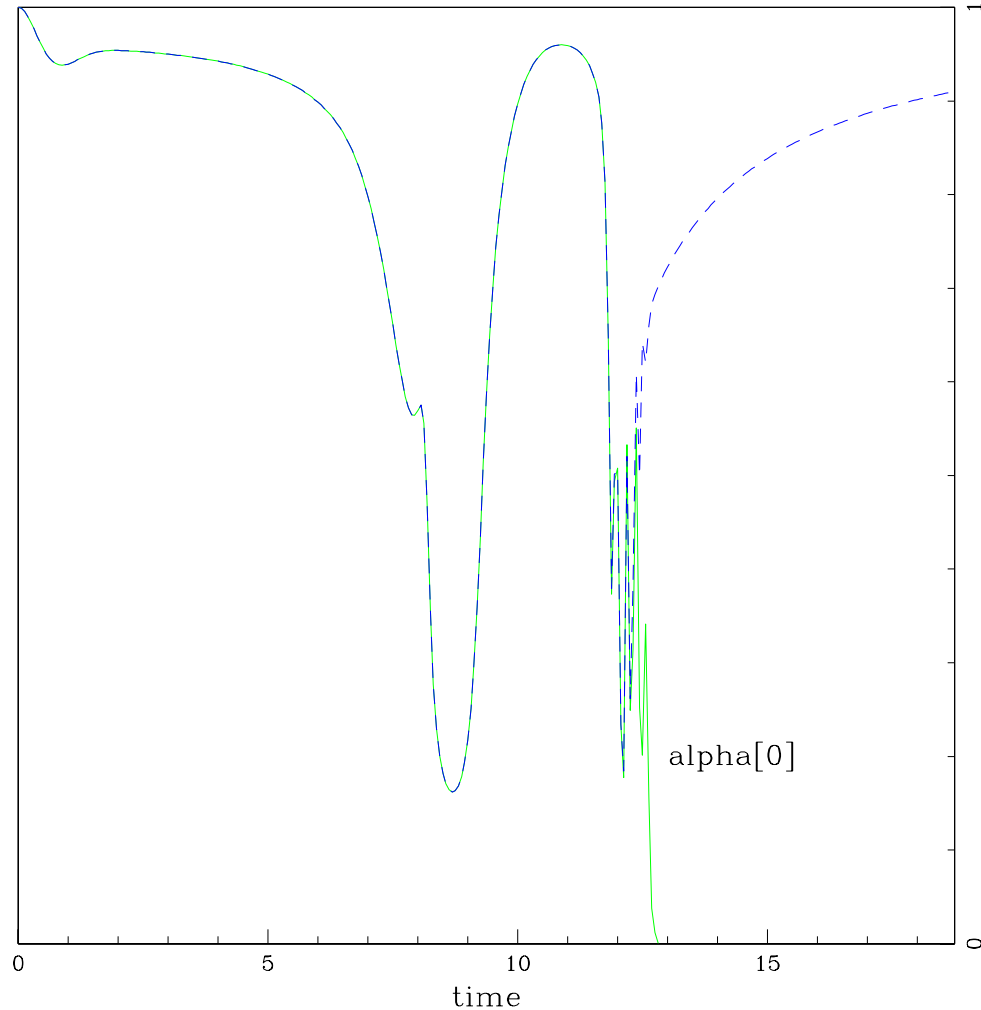


Figure 8.7 — Time plot of $\alpha|_{\rho=0}$ for supercritical (solid line) and subcritical (dashed) evolutions. The bouncing at the point of decision gets quite violent before the (slightly greater) wave forms a black string while the other disperses harmlessly away.

Chapter 9

Some Final Words

9.1 Cosmological Considerations

In an episode of *The Simpsons*, Stephen Hawking is talking to Homer Simpson in Moe's tavern. Says Hawking to Homer, "Your theory of a donut-shaped universe is intriguing. I may have to steal it." [33] Perhaps Matt Groening, *et al.*, were on to something there: the work presented herein made no stipulations about the size of the extra dimension relative to our submanifold.

Black strings, the result of gravitational collapse in 4+1 dimensions, are fascinating objects of study and may yet have more to reveal about our universe. Far from their original conception in the tenfold universe of planckoscopic string theory, black strings may describe large objects, from Cygnus X-1 to the supermassive black hole supposed to exist at the core of our own galaxy. Furthermore, if black holes are actually the four-dimensional projections of five-dimensional black strings, this has stunning implications for more mundane objects such as our sun, our planet, or even our own bodies: if our universe has an unseen dimension, it would be expected that black strings are not the only things to have an extension into the larger manifold.

9.2 Future Work

Clearly, "the field [of numerical gravitational collapse with an extra spatial dimension] is white, already to harvest" (D&C 4:4). One simple question, so obvious

I am astonished and even a little embarrassed that we did not think to address it earlier, concerns $\sigma_0 < 0$; all of our runs were for *positive* σ_0 . Since the actual metric component at issue is $g_{\zeta\zeta} = e^{2\sigma}$, a $\sigma_0 < 0$ would imply that the distortion in the extra dimension would be a compression instead of a spatial rarefaction. It would be interesting to explore the negative- σ regime to see if black strings still form, and whether the σ -black-string phase space exhibits interesting structure in the negative regime, or even an as-yet-undetected symmetry with respect to $\sigma_0 = 0$.

In addition, there are a number of assumptions we were forced to make for the sake of expediency which, in an expansion of the techniques utilized herein, may be done away with for a more in-depth examination. For instance, the astute reader will have noted that we began this thesis speaking of “black pearl necklaces,” or the question of whether black strings will multifurcate into an array of independent black holes. However, our assumption of the Killing vector $\xi = \partial_\zeta$ rendered the extra dimension inoperative, with its only effect—which nonetheless turned out to be substantial—being found in the term it contributes to the metric. Clearly, further work is possible, and necessary, wherein this Killing vector is not imposed and the numerical work done on a two-dimensional $\rho - \zeta$ grid.

The type of matter we chose to work with was the simplest of all, the massless scalar field. Unfortunately, it is also the hardest to physically identify; when one thinks of “matter” collapsing into a black hole one usually has in mind such things as dust and fluid—more physically realizable, naturally, but also much harder to work with in the equations. Thus, using a more pedestrian type of matter in the stress-energy tensor may be an interesting venture.

On the other hand, more exotic forms of matter and energy might also yield interesting results—say, forming a black hole entirely out of light (electromagnetic fields) or the truly exotic Yang-Mills field. One potent question regarding the latter

impinges upon work done by Millward and Hirschmann [34] of BYU, demonstrating that the YM field persists outside the black hole formed thereof in apparent violation of the classical “no-hair” theorem. The addition of an extra dimension to this work could yield some fascinating insights.

We assumed at the outset to be working in a universe of zero cosmological constant, despite the compounding evidence [29] that ours is a universe of $\Omega_\Lambda \sim 0.7$. Therefore, if one were to seriously wish to use higher-dimensional gravitation to predict and/or explain variances in astronomical black hole data from the expectation, inclusion of a nonzero Λ in the Einstein equations would be a must.

It could be that the self-similarity we caught a hint of is not limited to gravitational field collapse (*i.e.*, of pure σ distortions); after all, we did have to delve into the tenth decimal place to see it! We would not be surprised to find self-similarity that close to a scalar field collapse as well. It may also be an interesting course of research to determine, on a theoretical basis, the reason for the self-similarity observed numerically. Along with that, we would hope for an explanation of why the critical point takes on the value we found, and explanations of α 's critical kink (Fig. 8.6) and of its passage through a single point in its phase-space, regardless of the initial amplitude of σ .

9.3 Summary and Conclusion

Fascinating as those issues are, in this work, however, we chose to focus on the simple questions pertaining to black string formation via gravitational collapse in the first place. After all, better to have in hand some indication of black strings which one may search for, before wondering if one's own body occupies more dimensions than is commonly assumed. Our investigation, then, required solving the Einstein equations in 5-D, best done under the assumption of symmetries which we enforced

and explored via Killing vectors.

The spherical Killing vectors revealed a functional form for metric (and other tensor) components that forced a choice between two appealing approaches. The first approach proved a mistake, however, as shown (*ex post facto*) by careful consideration of what the Killing-revealed functionalities implied for equation-regularity. Dividing out spherical symmetry at first may sound like a good idea, but in doing so one encounters singular terms that cannot be transformed away. Numerical relativists everywhere ought to take note of this revelation.

Simplifying matters with a gauge choice, and sacrificing one question (regarding black string stability) to efficiently answer others (regarding gravitational field collapse), we discovered the mind-bending possibility of black strings made entirely of gravity. These begin as a spherical “shell” configuration of what appears (in a *gedanken* context, anyway) to be a *longitudinal* gravitational wave, or more precisely as a spherically symmetric local distortion in the extra dimension. We played exclusively with stretching (or as acousticians would call it, rarefaction); an initial compression (or negative σ) would make a fascinating additional study, as noted in (§ 9.2) above.

If we may use the classic trampoline mental illustration of general relativity’s curved spacetime, it is as if we stretched out spacetime in a narrow ring about the origin, then let it go. To our satisfaction if not astonishment, as in regular scalar field collapse, the local distortion bifurcates into outgoing and ingoing pulses. The ingoing portion increases in amplitude until the trampoline itself is rent at the center, signifying a black hole/string. The formerly ingoing wave, or the part of it that didn’t get sucked into the singularity, radiates away.

Even more amazing, however, is that if the initial stretching of spacetime is just right, or within millionths of a percent of being “just right,” the reflection of the

ingoing wave exhibits a self-echoing pattern characteristic of self-similarity. According to [32] this is no illusion; what remains a mystery is the theoretical basis for this behavior. Also intriguing, and remaining a mystery for the present time, is why smaller initial-amplitude distortions collapse faster than their larger counterparts.

This work opens the way, we think, to a wider world which physicists would be wise to explore more earnestly. Between this work and [32], and previous [1-31] and subsequent research (§ 9.2, above), we begin to understand what kinds of things one expects to find in “a donut-shaped” universe.

This includes the possibility of black holes made of nothing but a wrinkle in spacetime. The formation of such, if close to the critical value (and our present work offers no opinion as to whether critical collapse is some kind of “attractor” in black string phase space), would be marked by a distinctive self-similar radiative signature.

One might also wonder, since the Big Bang is a sort of reverse-collapse, if we might see echoes of self-similarity in the residual evidence of the founding event of the universe. Thus, black strings may hold the very key to the physical answer of man’s eternal question, Where did all of this come from?

Appendix A

Fun with conformal metrics

From the trace-free portion of the ADM equation for the time derivative of the slice metric we can discover what turns out to be a useful fact.

Let there be a metric that is conformal to our slice metric, *i.e.*, $\gamma_{AB} = \psi^{2p}\hat{\gamma}_{AB}$; $\gamma^{AB} = \psi^{-2p}\hat{\gamma}^{AB}$.

First of all, we note that since the contravariant metric (as a matrix) is defined as the cofactor of the covariant metric divided by the determinant thereof,

$$\gamma^{AB} \equiv \frac{\text{cof}(\gamma_{AB})}{\gamma},$$

then the time derivatives of γ and γ_{AB} are related thus:

$$\gamma^{AB}\partial_t\gamma_{AB} = \frac{1}{\gamma}\partial_t\gamma. \tag{A.1}$$

(The interested reader is invited to show this for him- or herself.)

With this in mind we contract (3.14) with γ^{AB} to find

$$\partial_t \ln(\gamma) = 2(\Delta_A \beta^A - \alpha K). \tag{A.2}$$

The trace-free portion of the $d = 4$ -dimensional spatial slice metric's time derivative is therefore (invoking (A.1)),

$$\partial_t\gamma_{AB} - \frac{1}{d}\gamma_{AB} \left(\gamma^{CD}\partial_t(\gamma_{CD}) \right) = \partial_t\gamma_{AB} - \frac{1}{d}\gamma_{AB} \left(\frac{1}{\gamma}\partial_t\gamma \right). \tag{A.3}$$

We then substitute (3.14) and (A.2) to obtain

$$\partial_t \gamma_{AB} - \frac{1}{d} \gamma_{AB} \left(\frac{1}{\gamma} \partial_t \gamma \right) = \Delta_A \beta_B + \Delta_B \beta_A - 2\alpha K_{AB} - \frac{2}{d} \gamma_{AB} \left(\Delta_A \beta^A - \alpha K \right).$$

Here another interesting fact comes to our aid. For if we multiply $\partial_t \gamma_{AB} - \frac{1}{d} \gamma_{AB} \left(\frac{1}{\gamma} \partial_t \gamma \right)$ by unity in the form of $\gamma^{\frac{1}{d}} \gamma^{-\frac{1}{d}}$ and distribute the negative power of γ we have before our eyes the time derivative of $\gamma^{-\frac{1}{d}} \gamma_{AB}$, multiplied by the remaining d^{th} root of γ . Therefore,

$$\gamma^{\frac{1}{d}} \partial_t (\gamma^{-\frac{1}{d}} \gamma_{AB}) = -2\alpha K_{AB} + \Delta_A \beta_B + \Delta_B \beta_A - \frac{2}{d} \gamma_{AB} \left(\Delta_A \beta^A - \alpha K \right). \quad (\text{A.4})$$

Now, since γ is the determinant of γ_{AB} there is a relationship between it and the determinant of the conformal metric, $\hat{\gamma}$:

$$\begin{aligned} \gamma &= \det(\gamma_{AB}) \\ &= \det(\psi^{2p} \hat{\gamma}_{AB}) \\ &= \psi^{2dp} \hat{\gamma}. \end{aligned}$$

Therefore, the combination $\gamma^{-\frac{1}{d}} \gamma_{AB}$ may be rewritten in terms of the conformal metric:

$$\begin{aligned} \gamma^{-\frac{1}{d}} \gamma_{AB} &= \left(\psi^{2dp} \hat{\gamma} \right)^{-\frac{1}{d}} \psi^{2p} \hat{\gamma}_{AB} \\ &= \hat{\gamma}^{-\frac{1}{d}} \hat{\gamma}_{AB} ! \end{aligned} \quad (\text{A.5})$$

Thus we see that the combination (A.5) is *conformally invariant*. This is the aforementioned useful fact: if we can replace $\gamma^{-\frac{1}{d}} \gamma_{AB}$ with *any* conformally equivalent combination, there is nothing to stop us from using coordinates such that $\gamma_{AB} = \psi^{2p} \hat{\gamma}_{AB}$, and choosing a $\hat{\gamma}_{AB}$ that is as simple as reason and good judgment will permit.

Along the abandoned road of our first approach (using s), we found that indeed there *was* a coordinate choice we could make that rendered $\hat{\gamma}_{AB} = \delta_{AB}$, as simple as one might hope. We will stop short of actually implementing the conformal transformation, but content ourselves with the knowledge that it is possible.

Given this fact, then, by conformal invariance, the LHS of (A.4) vanishes! We are thus left with an almost-elegant explicit equation for K_{AB} that is much easier dealt with than the more abstract and elusive “projection of the covariant derivative of n_μ ”:

$$K_{AB} = \frac{1}{4}\gamma_{AB}\left(K - \frac{\Delta_C\beta^C}{\alpha}\right) + \frac{1}{\alpha}\Delta_{(A}\beta_{B)}. \quad (\text{A.6})$$

(The parentheses around the indices in the final term denote symmetrization in the usual way.) This used to come in very handy in filling out the ADM equations until we decided that \tilde{K}_ρ^ρ , Ω , and a slicing condition were sufficient.

Bibliography

- [1] Th. Kaluza, *Sitzungsberichte der K. Preussischen Akademie der Wissenschaften zu Berlin*, 966 (1921); O. Klein, *Z. Physik* **37** 895 (1926).
- [2] E. G. Floratos, G. K. Leontaris, *Low Scale Unification, Newton's Law and Extra Dimensions*, *Phys. Lett.* **B465**, 95-100 (1999).
- [3] S. O. Mendes, R. Opher, *Sub-mm gravity: confronting the modified dynamics with higher-dimensional theories*, *Phys. Lett.* **B522**, 1 (2001).
- [4] L. Randall and R. Sundrum, *A Large Mass Hierarchy from a Small Extra Dimension*, *Phys. Rev. Lett.* **83**, 3370 (1999).
- [5] L. Randall and R. Sundrum, *An Alternative to Compactification*, *Phys. Rev. Lett.* **83**, 4690 (1999).
- [6] P. Matthews, S. Raychaudhuri, and K. Sridhar, *Large extra dimensions and deep-inelastic scattering at HERA*, *Phys. Lett.* **B455**, 115-119 (1999).
- [7] N. Arkani-Hamed, S. Dimopoulos, G. Dvali, and J. March-Russell, *Neutrino Masses from Large Extra Dimensions* *Phys. Rev.* **D65**, 024032 (2002).

- [8] T. Shiromizu, K. Maeda, and M. Sasaki, *The Einstein Equations on the 3-Brane World*, Phys. Rev. **D62**, 024012 (2000).
- [9] M. Parry, S. Pichler, *New bulk scalar field solutions in brane worlds*, JCAP **0411** 005 (2004).
- [10] R. A. Battye, A. Mennim, *Multiple-scales analysis of cosmological perturbations in brane-worlds*, Phys. Rev. **D70** 124008 (2004).
- [11] W. Israel, *Singular Hypersurfaces and Thin Shells in General Relativity*, Nuovo Cimento **44B**, 1 (1966).
- [12] E. W. Hirschmann and A. Wang, unpublished work, Brigham Young University (2002).
- [13] R. Gregory and R. Laflamme, *Black Strings and p-Branes are Unstable*, Phys. Rev. Lett. **70**, 2837 (1993).
- [14] R. Gregory and R. Laflamme, *The Instability of Charged Black Strings and p-Branes*, Nucl. Phys. **B428**, 399 (1994).
- [15] G. T. Horowitz, J. M. Maldacena, and A. Strominger, *Nonextremal Black Hole Microstates and U-duality*, Phys. Lett. **B383**, 151 (1996).
- [16] N. Itzhaki, J. M. Maldacena, J. Sonnenschien, and S. Yankielowicz, *Supergravity and The Large N Limit of Theories With Sixteen Supercharges*, Phys. Rev. **D58**, 046004 (1998).
- [17] O. Aharony, S. S. Gubser, J. M. Maldacena, H. Ooguri, and Y. Oz, *Large N Field Theories, String Theory and Gravity* Phys. Rept. **323**, 183 (2000).

- [18] G. T. Horowitz and V. E. Hubeny, *Quasinormal Modes of AdS Black Holes and the Approach to Thermal Equilibrium*, Phys. Rev. **D62**, 024027 (2000).
- [19] G. T. Horowitz and K. Maeda, *Fate of the Black String Instability*, Phys. Rev. Lett. **87** 131301 (2001).
- [20] D. Marolf, *On the fate of black string instabilities: An Observation*, as yet unpublished; [arXiv:hep-th/0504045].
- [21] G. T. Horowitz, private communication with E. W. Hirschmann (2001).
- [22] M. W. Choptuik, L. Lehner, I. Olabarrieta, R. Petryk, F. Pretorius, and H. Villegas, *Towards the Final Fate of an Unstable Black String*, Phys. Rev. **D68**, 044001 (2003).
- [23] M. W. Choptuik, *Universality and scaling in gravitational collapse of a massless scalar field*, Phys. Rev. Lett. **70**, 912 (1993).
- [24] A. Wang, *Critical Phenomena in Gravitational Collapse: The Studies So Far*, Braz.J.Phys. **31** 188-197 (2001).
- [25] M. W. Choptuik, personal communication to E. W. Hirschmann (2003).
- [26] L. Witten, "The Dynamics of General Relativity," *Gravitation: An Introduction to Current Research*, (Wiley, New York, 1962).
- [27] R. L. Spencer, instructor: *Physics 441*, **C266** ESC (Fall semester, 1999).
- [28] R. d'Inverno, *Introducing Einstein's Relativity*, Oxford University Press, 169-170 (1998).

- [29] S. Perlmutter, *et al.*, *The Supernova Cosmology Project* *Astrophys. J.* **517** 565 (1999). See also <http://www-supernova.lbl.gov/> .
- [30] R. d’Inverno, *Introducing Einstein’s Relativity*, Oxford University Press, 189 (1998).
- [31] S. A. Hayward, *Black holes: new horizons*, Brief talk given to open the Generalized Horizons session of the Ninth Marcel Grossmann Meeting, Rome, July 2000; [arXiv:gr-qc/0005126].
- [32] P. Bizoń, T. Chmaj, and B. G. Schmidt, *Critical behavior in vacuum gravitational collapse in 4 + 1 dimensions*, as yet unpublished; [arXiv:gr-qc/0506074].
- [33] M. Groening, J. L. Brooks, I. Maxtone-Graham, *et al.*, *They Saved Lisa’s Brain*, *The Simpsons*, **AABF18** (1999).
- [34] R. S. Millward and E. W. Hirschmann, *Critical behavior of gravitating sphalerons*, *Phys. Rev.* **D68** 024017 (2003).